INFORMATION TO USERS

This dissertation was produced from a microfilm copy of the original document. While the most advanced technological means to photograph and reproduce this document have been used, the quality is heavily dependent upon the quality of the original submitted.

The following explanation of techniques is provided to help you understand markings or patterns which may appear on this reproduction.

1. The sign or "target" for pages apparently lacking from the document photographed is "Missing Page(s)". If it was possible to obtain the missing page(s) or section, they are spliced into the film along with adjacent pages. This may have necessitated cutting thru an image and duplicating adjacent pages to insure you complete continuity.

2. When an image on the film is obliterated with a large round black mark, it is an indication that the photographer suspected that the copy may have moved during exposure and thus cause a blurred image. You will find a good image of the page in the adjacent frame.

3. When a map, drawing or chart, etc., was part of the material being photographed the photographer followed a definite method in "sectioning" the material. It is customary to begin photoing at the upper left hand corner of a large sheet and to continue photoing from left to right in equal sections with a small overlap. If necessary, sectioning is continued again — beginning below the first row and continuing on until complete.

4. The majority of users indicate that the textual content is of greatest value, however, a somewhat higher quality reproduction could be made from "photographs" if essential to the understanding of the dissertation. Silver prints of "photographs" may be ordered at additional charge by writing the Order Department, giving the catalog number, title, author and specific pages you wish reproduced.

University Microfilms

300 North Zeeb Road
Ann Arbor, Michigan 48106

A Xerox Education Company

THE UNIVERSITY OF OKLAHOMA

GRADUATE COLLEGE

SOME ELECTRICAL AND TRANSPORT PROPERTIES OF TUMOR CELLS

A DISSERTATION

SUBMITTED TO THE GRADUATE FACULTY

in partial fulfillment of the requirements for the

degree of

DOCTOR OF PHILOSOPHY

BY

ALEC CHI CHOU

Oklahoma City, Oklahoma

1972

SOME ELECTRICAL AND TRANSPORT PROPERTIES OF TUMOR CELLS

APPROVED BY

DISSERTATION COMMITTEE

TO MY FATHER,

MY WIFE, FUANG-HUEI and

DAUGHTER, STEPHANIE

ACKNOWLEDGMENT

The author wishes to take this opportunity to express sincere appreciation to Dr. Tushar K. Chowdhury for his guidance, encouragement and financial support which greatly aided the completion of this study. His patience and help in preparing this dissertation are gratefully acknowledged.

Special gratitude is due to Dr. A. Kurt Weiss for his concern, encouragement and helpful suggestions during this study. The author is also grateful to Drs. A. C. Cox, M. J. Keyl and R. Thies for their helpful suggestions in the preparation of this dissertation.

The author is thankful to Drs. G. M. Kollmorgen and L. R. Miller for their generous help in establishing the initial tissue culture system. Appreciation is also due to Dr. L. M. Lin for his invaluable assistance in interpreting the histopathology of the tumor tissues.

The technical assistance of Mr. R. R. Langley is highly appreciated. The author is indebted to Mrs. Eileen Spain for her help in typing this dissertation.

My research has been performed in the Department of Physiology and Biophysics, University of Oklahoma Health Sciences Center, and was supported by NSF research grant GB18726.

TABLE OF CONTENTS

	Page
LIST OF TABLES	vi
LIST OF ILLUSTRATIONS	vii
Chapter	
I. INTRODUCTION	1
II. METHODS AND MATERIALS	18
III. RESULTS	35
IV. DISCUSSION	85
V. SUMMARY	96
BIBLIOGRAPHY	99
APPENDIX	108

LIST OF TABLES

Table		Page
1.	Composition of the Medium B_1D.....	21
2.	Compositions of Various Solutions.....	22
3.	The Amino Acid Uptake Studied with an Amino Acid Analyzer.....	60
4.	The Effects of DNP and Iodoacetate on Glycine, Phenylalanine and Histidine Uptake in Anaplastic Carcinoma Cells....	79
5.	The Effects of α-MG on Con A Inhibition of Glycine Uptake.....	83
6.	The Effects of α-MG on Con A Inhibition of Phenylalanine Uptake.....	84

LIST OF ILLUSTRATIONS

Figure — Page

1. Block Diagram of Recording Apparatus for Electrical Measurement..... 28

2a. Histology of Chemically Induced-Skin Tumor (I)..... 37

b. High-magnification of Histology of Chemically Induced-Skin Tumor (I)..... 37

3a. Histology of Chemically Induced-skin Tumor (II)..... 39

b. High-magnification of Histology of Chemically Induced-Skin Tumor (II)..... 39

4a. Histology of Transplantable Mouse Tumor..... 41

b. High-magnification of Histology of Transplantable Mouse Tumor..... 41

5a. The Transplantable Anaplastic Carcinoma Cells in Tissue Culture Observed Under a Phase Contrast Microscope (320x).. 44

b. High-magnification of the Transplantable Anaplastic Carcinoma Cells in Tissue Culture Observed Under a Phase Contrast Microscope (640x)..... 44

6a. The Cultured Fibroblasts from Subcutaneous Tissue of Normal A/J Mouse Observed under a Phase Contrast Microscope (320)..... 46

b. High-magnification of the Cultured Fibroblasts from Subcutaneous Tissue of Normal A/J Mouse Observed Under a Phase Contrast Microscope (640x)..... 46

7. The Growth Curve of Anaplastic Carcinoma Cells in Tissue Culture..... 48

8. The Relationship Between Resistance of Microelectrode and Magnitude of Tip Potential Change Caused by Placing the Microelectrode from K-Ringer's Solution to Na-Ringer's Solution..... 50

9. The Relationship between Intrinsic Tip Potential of Microelectrode and Magnitude of Tip Potential Change Caused by Placing the Microelectrode from K-Ringer's Solution to Na-Ringer's Solution..... 51

10. Polygraph Recordings of Intracellular Potential and Membrane Resistance of Skin Tumor Cells in Mouse Ringer's Solution.. 53

LIST OF ILLUSTRATIONS - Continued

Figure | Page

11. The Intracellular Potentials of Normal and Tumor Cells of the Skin of Mice (C3H strain)..... 56

12. The Membrane Resistance of Normal and Tumor Cells of the Skin of Mice (C3H strain)..... 57

13. The Saturation Curves for Glycine (●— — —), Phenylalanine (▲---) and Histidine (◇——) Uptake in Anaplastic Carcinoma Cells..... 62

14. Effects of Con A on Glycine Uptake in Normal Fibroblasts and Anaplastic Carcinoma Cells..... 63

15. Effects of Con A on Phenylalanine Uptake in Normal Fibroblasts and Anaplastic Carcinoma Cells..... 64

16. Effects of Con A on Histidine Uptake in Normal Fibroblasts and Anaplastic Carcinoma Cells..... 66

17a. The Anaplastic Carcinoma Cells in Tissue Culture Observed under a Phase Contrast Microscope Prior to Con A Incubation (320x)..... 68

b. The Anaplastic Carcinoma Cells in Tissue Culture Following 1 Hour of Incubation with 750 µg/ml Con A and 1 Hour of Incubation with Medium B_1D..... 68

18. The Effects of Con A on Growth Curves of Anaplastic Carcinoma Cells in Culture..... 69

19. Effects of Polylysine on Glycine Uptake in Normal Fibroblasts and Anaplastic Carcinoma Cells..... 70

20. Effects of Polylysine on Phenylalanine Uptake in Normal Fibroblasts and Anaplastic Carcinoma Cells..... 72

21. Effects of Polylysine on Histidine Uptake in Normal Fibroblasts and Anaplastic Carcinoma Cells..... 73

22a. The Anaplastic Carcinoma Cells in Tissue Culture Observed Under a Phase Contrast Microscope Prior to Polylysine Incubation (320x)..... 75

b. The Anaplastic Carcinoma Cells in Tissue Culture Following 10 Min Incubation with 150 µg/ml Polylysine and 1 Hr Incubation with Medium B_1D..... 75

LIST OF ILLUSTRATIONS - Continued

Figure | Page

23. The Follow-up Picture of Figure 22b..... 77

24. High-magnification Photomicrograph of Anaplastic Carcinoma Cells in Tissue Culture after a 10 Min Incubation with 300 µg/ml Polylysine and 1 Hr Incubation with Medium B_1D (640x)..... 77

25. The Effects of Temperature on Amino Acid Uptake in Anaplastic Carcinoma Cells..... 80

26. A Replot of Figure 25..... 82

27. A Model Illustrating the Difference Between the Cell Surface of a Normal Mouse Fibroblast and an Anaplastic Carcinoma Cell, Particulary with Respect to the Relative Location of the Amino Acid Transport Sites to the Con A and Polylysine Binding Sites on the Membrane Surfaces.... 92

SOME ELECTRICAL AND TRANSPORT PROPERTIES OF TUMOR CELLS

CHAPTER I

INTRODUCTION

In reviewing the work done on cancer cell membranes during the last four decades, it is likely that in many cases the alteration of plasma membrane plays a key part in neoplasia. Although evidence in support of this view comes from widely dispersed observations, none of the many biological, biochemical, immunological and morphological defects hitherto described are common to all tumors (1).

In 1944, Coman (2) demonstrated that mutual adhesion was much less between carcinoma cells than between normal epithelial cells. This finding was considered by Coman and later on by Ambrose (3) to explain the invasion and metastasis of malignant cells.

Beginning in 1953, Abercrombie and his co-workers (4, 5, 6) made a series of studies observing the differences between the social behavior of normal fibroblasts and sarcoma cells in tissue culture. Normal fibroblasts affect each others' movement by contact inhibition, whereas sarcoma cells do not manifest inhibition either between themselves or between sarcoma cells and normal fibroblasts. The loss of contact inhibition was also shown by Temin and Rubin (7) in experiments utilizing oncogenic viruses for malignant transformation of fibroblasts. However, contact

inhibition is sometimes exhibited even among malignant cells and yet not by some normal cells (8). Curtis (9) has also demonstrated that nutrients in the medium can affect the social behavior; the contact inhibition is partially lost in fibroblasts when the amount of chick embryo extract in the culture medium is increased beyond a certain level. Therefore, loss of contact inhibition cannot be regarded as a universal characteristic of tumor cells.

The attempt to compare the surface charge of malignant cells of solid tumors with their normal analogues was made by Ambrose et al. (10) and Lowick et al. (11). They showed that malignant cells from a hamster kidney tumor and a rat hepatoma had higher electrophoretic mobilities than their normal counterparts. Purdom et al. (12) also demonstrated a positive correlation between electrophoretic mobilities and invasiveness in the various strains of the murine MCIM sarcoma. Ambrose (3) has suggested that an increased negative charge density on the surface of tumor cells results in an electrostatic repulsion between them and hence the loss of adhesiveness. The invasiveness of tumor cells has been attributed to this loss of cell adhesiveness.

On the other hand, other studies have indicated that increased surface charge is not a general characteristic of tumor cells. First of all, Ben-Or et al. (13) showed that the electrophoretic mobilities of isolated cells from regenerating normal rat liver were higher than their normal counterparts. This observation suggested that increased surface charge density is probably a phenomenon common to growth process in general. Secondly, Doljanski (14) reported that the electrophoretic mobilities of leukemia cells and Rous sarcoma virus (RSV)-transformed chick

fibroblasts both were similar to those of their normal analogues. Thirdly, Ohta et al. (15) demonstrated that the sialic acid contents of three lines of virus-transformed tumor cells were consistently lower than normal cells. This is contrary to what might be expected since the surface negative charge is generally considered to be due to sialic acid. Finally, Weiss (16) analysed the results obtained by different isolation techniques and emphasized the possibility of a cellular breakage artefact in preparing the cells for electrophoresis in all of the previous studies.

Therefore, it appears that although the membrane alteration is a regular feature of neoplasia, because of the individuality and pleiomorphism, the property of tumor cells has so far not been characterized by any single manifestation of membrane alteration. It seems that some other new approaches would be highly desirable in understanding the nature of the tumor cells.

Transport of nutrients and electrolytes across cell membrane plays an important role in supplying the substrates needed for the synthesis of various substances as well as the maintenance of cellular metabolism and osmotic balance. Since cancer is generally a disorder of growth, some alterations in the transport processes are to be expected. One of approaches to detect the alteration in the transport of electrolytes in cancer is a comparative determination of the intracellular potential and membrane resistance of cancer cells versus normal cells. Whether cancer cells have any inherent defect in their uptake of one of the most needed class of nutrients, e.g., amino acids, can be determined very effectively with the aid of radioactive tracer techniques.

Intracellular Potential and Membrane Resistance

There have been only a few measurements of the intracellular potential of malignant cells, especially of cells in culture. Borle and Loveday (17) reported that the intracellular potential of HeLa cells had a mean value of -15mV in growth medium. Johnstone (18) obtained both positive and negative potentials on penetration of Ehrlich ascites tumor cells. He assumed that the former might be due to potential difference between the cytoplasm and the external medium, and the latter might occur on the penetration into some internal structures of the cell. Aull (19) found that Ehrlich ascites tumor cells in Ringer's solution had a mean potential of -11.2 mV. Very recently the recordings of the intracellular potentials of cells infected in vitro with viruses were reported (20). Non-infected human lung fibroblast cells displayed negative polarity, whereas cells infected with herpes simplex virus type 1 or type 2, or cytomegalovirus, displayed a shift to positive polarity. Besides, the malignant HEp-2 cells also showed the same shift after infection. It has been suggested that the reversal of polarity was a result of infection with viruses. Exactly how this can happen is unknown.

Because of the lack of potential measurements in normal counterparts, most of the potential measurements from single malignant cells do not give much information about the magnitude and nature of the alteration of electrical properties of the tumor cells. The comparison between the intracellular potentials of normal and malignant cells is at present available only in a few cases, largely by in situ study in which the probing of cells was performed in the presence of other constituents of the whole tissue. In most cases, the potentials in the malignant cells

are lower than those of their corresponding normal cells.

Similarly, the processes occurring in changing membrane resistance in malignancy are scantily documented. In the in situ studies, Loewenstein and his associates (21, 22, 23) compared the membrane resistances of the malignant rat liver and thyroid cells of various animals (rat, hamster, mouse and man) with their homologous normal cells. They showed that the resistances of both the junctional and non-junctional membrane of the cancer cells were higher than those of the normal cells. Their in vitro study (24) displayed the same trend of resistance changes with epithelial cells, but the resistances of normal and malignant fibroblasts were similar.

On the contrary, Sheridan (25) found low resistance intracellular junctions, as revealed by electrical coupling between cells, in four types of tumors, sarcoma 80, Novikoff hepatoma, and Morris hepatomas 3924-A and 7777, although no absolute value of the membrane resistance was given.

As can be seen from the survey presented, the intracellular potential and membrane resistance have been measured on a comparative basis only in a limited number of cells. One of the purposes of the present study is to extend such electrical measurements to other kinds of cells and with a greatly refined technique. Two widely different groups of cells are chosen for this purpose. The first group is composed of the normal epithelial cells of the skin and the corresponding cancerous cells induced purely by chemical means. The second group consists of the normal fibroblasts of subcutaneous tissue and the corresponding transplantable anaplastic carcinoma cells.

Amino Acid Transport in Tumor Cells

The experimental observation that amino acids are maintained in animal cells at much larger concentrations than in the plasma was made as early as 1913 by Van Slyke and Meyer (26). They showed that after an injection of amino acid solutions into an animal, the concentration of amino acids in the liver cells rose higher than the level of plasma concentration. *In vitro* studies of uptake of the amino acids by isolated organ slices were started in 1949. In that year Christensen and Streicher (27) and Christensen *et al.* (28) showed that the diaphragm is capable of transporting and accumulating amino acids, and Stern *et al.* (29) demonstrated an accumulation of glutamate by rat brain slices. Wiseman (30) and Fridhandler and Quastel (31) used the intestinal preparations for studying transfer of amino acids across the intestinal wall. Red blood cells and reticulocytes were the first type of animal cells to be used in cell suspension for amino acid transport (32, 33). Most of the earlier work of amino acid transport in cancer cells was performed on Ehrlich ascites tumor cells, which have the ability to concentrate many amino acids (34, 35).

Many general characteristics of the amino acid transport system have been established in studies with Ehrlich ascites tumor cells. However, in order to make a valid comparison, the possibility that amino acid transport is altered in association with malignancy requires also a knowledge of the transport process in the normal cells. Eagle *et al.* (36) found no differences in the ability of several cultured human cell lines derived from normal and malignant tissues to accumulate amino acids. Also, Hare (37) found no significant changes in the characteristics of

L-phenylalanine transport by virus-transformed neoplastic hamster cells. However, Foster and Pardee (38) observed that polyoma virus-transformed 3T3 cells accumulated α-aminoisobutyric acid (AIB), cycloleucine, and glutamine about twice as rapidly as the untransformed 3T3 cells. Kinetic analysis suggested that the transformed cells had higher transport maxima for AIB and cycloleucine. Comparable to the findings of Foster and Pardee, Isselbacher (39) recently observed a 2.5 to 3.5-fold increase in the rate of uptake of these substances in transformed cells as compared to the normal cell lines. In addition, the rates of uptake of arginine and glutamic acid were similar to those with AIB and cycloleucine. Also noted were the increased rates of uptake of AIB and cycloleucine by liver cells transformed with MSV (mouse sarcoma virus) as compared with the normal cells. It appears, therefore, that the changes in transport in the virally transformed cells might be due to an alteration at the level of cell membrane. Thus, a study of the effects of surface interacting agents on amino acid uptake may be helpful in understanding the nature of transport sites.

Inbar et al. (40) demonstrated that the transport of amino acids, namely leucine, arginine, glutamic acid, glutamine, AIB and cycloleucine in the transformed cells was inhibited by Con A (concanavalin A), but no inhibitory effect of Con A was observed in the normal cells. They suggested that malignant transformation of normal cells resulted in a change in the location of amino acid transport sites in the surface membrane in relation to the binding sites of Con A. This work is interesting especially relating to Burger's finding (41) that polyoma virus transformed mouse fibroblasts treated with Con A restored the normal growth pattern.

Structure of Concanavalin A and Some of Its Suggested Biological Effects

In 1919 Sumner (42) isolated a hemagglutinin from jack beans and named it concanavalin A (Con A). This crystalline Con A had an isoelectrical point of pH 5.5, a sedimentation coefficient of 6.0 and a molecular weight of 96,000, as reported later by Sumner and his co-workers (43, 44). Olson and Liener (45) reported that the product obtained by Sumner's method contained 4% carbohydrate.

In 1967 Olson and Liener (45) and Agrawal and Goldstein (46) developed new preparations which had been shown to give better purity. Carbohydrate was removed by treatment with 1 M acetic acid without any diminution of hemagglutinating or glycogen-precipitating activity. Further purification was achieved by selective adsorption on a Sephadex G-100 or G-50 column, followed by elution with dilute acid or D-glucose solution. The molecular weight of purified Con A based on ultracentrifugation data is near 70,000 at a pH between 7 and 8. No carbohydrate was present, as shown by the negative results with several colorimetric reactions for neutral, amino and acid sugars (46). In addition, the molecular weight value of 68,000 calculated from the amino acid composition was very close to the value of 71,000 obtained from the sedimentation equilibrium data (45). This indicated the absence of any appreciable amount of non-protein material. Since most of the phytohemagglutinins which have been isolated to date have been shown to be glycoprotein containing 5-10% carbohydrate, the absence of carbohydrate can either be a unique characteristic of the Con A structure, or imply the presence of impurity in the preparations of other phytohemagglutinins (45).

Gel electrophoresis and gel filtration performed by Wang et al. (47) further indicated that native Con A contained several molecular species. By ion-exchange chromatography, they isolated and characterized an intact subunit of molecular weight 27,000 as well as three other fragments of the intact subunit. The intact subunit appeared to have all the properties of Con A. They postulated that the intact subunit could bind other subunit(s) or fragment(s) to form either a dimer as seen at a pH lower than 5.8 or to form a tetramer at neutral pH. This hypothesis explained well the wide variation of molecular weights obtained from earlier studies. Abe et al. (48) using different procedures also obtained 3 major components, α, β_1 and β_2 of Con A preparations with molecular weight 27,000, 16,000 and 13,000 respectively. Chemical studies on the isolated components confirmed the oligomer hypothesis; the αcomponent denoting the intact subunit, and β_1 and β_2 corresponding to two halves of a polypeptide chain of the subunit.

N.B.: Proposed relationship between an intact subunit (α) and fragments (β_1 & β_2).

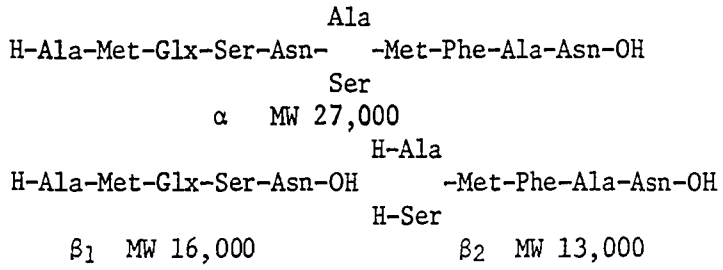

The fact that α/β ratios varied markedly according to the sources of the beans explained once again the reason for the variation in the molecular weight values.

The intact subunit contains binding sites for both metals and sugar (49, 50), and it has 2 methionyl residues at which cleavage takes

place during treatment with cyanogen bromide. The three CNBr fragments (F1, F2, & F3) have been isolated from the subunit and characterized (51). The data on amino acid composition of the intact subunit and fragments under different experimental conditions have also been reported (47, 48, 51).

X-ray diffraction studies performed by Hardman et al. (52) and Quiocho et al. (53) demonstrated the tertiary structure of the Con A molecules. The crystal was orthorhombic with unit cell dimensions of 63, 87, and 89 Å. Hardman et al. showed that each unit cell contains eight asymmetric units. The asymmetric unit, protomer, had a molecular weight of 27,000 and reflected the unique chemical component within the oligomer. This observation was consistent with that of others that Con A had an intact subunit with a molecular weight of 27,000. The spatial relationship was clearly illucidated in the electron density map. Near pH 7, four asymmetrical units (synonymous with intact subunit in the paper of Wang et al.) clustered around the intersection of three mutually perpendicular two-fold rotation axes to form a tetramer molecule of 108,000 daltons. Between pH 3 and 6, the molecule could be dissociated into dimers with 2 protomer units (MW 54,000).

In summary, Con A is a mixture of oligomers. At acidic pH dimers predominate, while at neutral pH a tetramer is the major entity. The dimer and tetramer are mainly composed of 2 and 4 identical subunits respectively, but the formation of a dimer by the combination of an intact subunit and its fragment or fragments also exists. The contribution of the later process varies widely with the method of preparation and source of material. The intact subunit contains binding sites to some

metal ions and carbohydrates and it has a molecular weight of 27,000. Chemical analysis showed that it is a polypeptide with alanine at the N and asparagine at the C-termini. The striking feature in amino acid composition analysis is that no cysteine or cystine was identified in polypeptide.

Con A has been shown to agglutinate erythrocytes of various animal species, yeast cells, starch granules and some bacteria (43). This protein had also been shown to be mitogenic for human and rabbit lymphocytes (54, 55). Furthermore, Con A inhibited phagocytosis of polymorphonuclear leukocytes (56) and migration of lymphoma and carcinoma TA3-NS cells (57). In certain specific cases, Con A was also shown to be able to precipitate various polysaccharides (43, 58).

However, interest in Con A has largely grown only recently as a result of the observations that variation in binding of Con A may reveal structural changes on membrane surfaces (59, 60), and due to the demonstration that Con A can restore the growth patterns of transformed fibroblasts to that of normal cells (41).

Changes in the cell surface have been postulated to be a basic phenomenon and one of the most typical characteristics of cancer cells (61, 62, 63, 64). The study of agglutination is important in the sense that it yields a convenient way to visualize the surface alteration. Beside Con A, the agglutinin isolated from wheat germ has been extensively studied (64, 65, 66). Like Con A, wheat germ agglutinin agglutinates malignant cells selectively. Furthermore, it can agglutinate the protease treated untransformed cells as the Con A does. The disadvantage of using wheat germ agglutinin is that the resulting agglutination can be overcome

by serum glycoproteins and serum, which are often the indispensable components of the culture medium (41, 67).

Inbar and Sachs (59) had made several important observations about Con A: 1) Con A can agglutinate leukemia cells and cells transformed by polyoma virus, Simian virus 40, chemical carcinogens, and X-irradiation, but it does not agglutinate normal cells; 2) the agglutination is reversed by competition with α-methyl-D-glucopyranoside (α-MG), a carbohydrate that strongly binds to Con A; 3) destruction of the α-MG binding sites of Con A abolishes the agglutination; 4) when non-agglutinable normal 3T3 cells are infected with Simian virus 40 or normal rat cells are infected with polyoma virus, the infected cells become agglutinable several days after infection; 5) trypsin treatment results in increasing agglutinability of normal hamster and 3T3 cells with Con A, whereas the agglutinability of the transformed cells is decreased. These results indicate that the surface membrane of malignant cells contains "sites" that interact with the α-MG binding sites of Con A, and that these "sites" are present in normal cells in cryptic form, and they can be exposed by treatment with protease.

Burger's work (68, 69) further supports the view that exposure of surface sites is closely linked to the unregulated growth of malignant cells. He observed that addition of small amounts of trypsin or pronase to a confluent 3T3 fibroblast culture caused a temporary escape of contact inhibition of growth, and eventually reaches densities at which some cells were overlapping with each other. On the other hand, polyoma virus transformed mouse fibroblasts (Py3T3) treated with monovalent Con A (trypsin splitted Con A) regained growth control, and the culture

reached the saturation density of normal 3T3 cells (41).

More direct evidence concerning the binding sites came from the experiment using Con A labelled with ^{63}Ni (67). This method enables the calculation of the number of sites per unit cell surface. The sites that interact with α-MG specific binding sites of Con A on the normal and transformed cells were compared. The transformed cell had more of these binding sites exposed on its surface than had the untransformed cell. After trypsin treatment of normal cells, the sites increased to a level similar to that found with transformed cells. The results indicated again that normal and transformed cells had a similar number of sites on the surface membrane that interact with the α-MG binding sites of Con A, while in normal cells a majority of these sites were in the cryptic form.

Despite convincing evidence provided by Inbar and Burger's groups, the idea that transformation involves an increase of Con A binding sites was challenged by the observations of Ozanne and Sambrook (70), and Cline and Livingston (71). Using Con A labelled with ^{125}I or ^{3}H, they showed that, while BHK and 3T3 cells transformed by polyoma and SV 40 viruses were more readily agglutinated than the corresponding untransformed cells, the transformed and untransformed cells bind about the same amounts of Con A on a per milligram protein basis. This observation indicated that there was no relationship between the number of Con A receptor sites on the cell surfaces and their degree of growth control or their agglutinability. Perhaps some more subtle mechanisms are involved on the cell surface, rather than just the exposure of Con A binding sites. Nevertheless, these studies confirm that the cell agglutinability by Con A did

increase in transformed cells.

In the present investigation well controlled tissue culture preparations of normal fibroblasts and anaplastic carcinoma cells will be used to test if indeed Con A shows any differential effects on the transport of some amino acids in these two systems.

Polylysine

Polylysine is a basic homopolyamino acid which exhibits a strong positive charge in the physiological pH range. It has some profound biological effects. Besides causing agglutination of erythrocytes (72, 73), Ehrlich ascites tumor (74) and leukemic cells (75, 76), polylysine also was shown to have antivirus, antibacteria and anticancer activities.

Polylysine decreases the virulence of tobacco mosaic virus (77), inhibits multiplication of bacteriophage (78, 79), and protects chick embryos from viruses such as mumps (80) and influenza B viruses (81). Burger and Stahmann (82) and Katchalski et al. (83) found that polylysine agglutinates bacteria and inhibits growth.

Richardson et al. (84) demonstrated that growth and division of the diploid strain of Ehrlich ascites carcinoma and TAB ascites carcinoma are markedly inhibited by polylysine. Shah and Reilly (85) reported that incubation of the mouse mammary tumor cells with polylysine and lysine-rich histone fractions before inoculation inhibited the growth of the tumor. Polylysine also reduces invasion by polyoma virus-transformed fibroblasts into fetal mouse explants in organ culture (86). Some other polycations were shown to have similar antitumor effect. Polyethylene imine interacts specifically with Walker tumor cells and not with erythrocytes or spleen cells (87). Larsen and Olsen (88) reported that

polyornithine inhibited the transplantability of mouse leukemia, whereas arginine-rich protamine sulphate failed to do so.

All the biological effects of polylysine described above probably are secondary to its primary action on the cell membranes. The fundamental reaction involves the electrostatic interaction between the polycation and the negative ionic groups of the cell surface (72). With red blood cells Katchālsky concluded that polylysine is bound to the membrane only (72). In addition, studies with fluorescent polylysine have demonstrated that polylysine binds to the lipoprotein surface of Ehrlich ascites tumor cells and does not penetrate the cell membrane to any appreciable extent at least within 10 min (74). The cellular agglutination is accordingly formed by the multiple bonds between polycation and two adjoining membranes; the polymer, in fact, serves as a bridge connecting cells on each side.

The nature of the interaction between basic polyelectrolytes and cell surfaces, however, is not known. A marked effect on the transport process of the tumor cell membrane was suggested by Kornguth and Stahmann (74). They showed that polylysine treated Ehrlich ascites tumor cells enhanced the release of small molecular weight materials such as nucleotides, amino acids, peptides, potassium, carbohydrate and phosphate, but the release of proteins and phospholipids were inhibited. In addition, Mangos and McSherry (89) demonstrated that polylysine inhibited sodium transport in the rat parotid gland. Sirica and Woodman (76) studied the polylysine effect on L1210 leukemia cells both *in vitro* and *in vivo*. They also attributed the cytoplasmic swelling and cytolysis produced by polylysine treatment to increased permeability. Based on the observation

that cytoplasmic swelling and cytolysis occurred when the polycation-treated cells were suspended in an isotonic saline environment, they suggested that the adsorption of cationic polyelectrolytes by the cell surface preceded a disruption of the structural integrity of the plasmalemma. The alteration of membrane conformation resulted in a change in permeability to solutes and mediated through osmotic swelling a mechanical rupture of the plasmalemma occurred.

It is interesting to note that on the one hand polylysine plays an inhibitory role in membrane transport, and yet on the other hand, it increases the uptake of albumin in sarcoma S-180 cells (90, 91) and induces pinocytosis in Amoeba proteus (92).

From the wide range of effects of polycation imposed on the membrane, it is evident that the interaction between the basic polyelectrolyte and the cell surface is not a simple one, but more likely it involves a delicate and specific process. Physicochemical studies of the membrane protein conformation has demonstrated that a significant part of the cell membrane protein is in the α-helical form (93). It was suggested that some of the α-helical segments of the protein molecule reach into the lipid bilayer, whereas other segments reside on the membrane surface. Ryser (90) suggested that polybasic compound interacting with the negative end groups of the cell surface might influence the conformation of membrane proteins by changing the charge distribution on segments of peptide chains. Multiple attachment to adjoining points of the membrane could strain the membrane structure. Profound effects on membrane structure and function are expected when one long chain polymer interacts with several structural proteins. Even though a number of investigators has studied

various types of effects of polylysine, none of them has directed any attention to the effect of this surface binding agent on the transport of amino acids. Therefore, in this investigation an attempt will be made to study the effects of polylysine on the amino acid uptake of anaplastic carcinoma cells and normal fibroblasts.

In reiteration, the general goal of this study is to find a better way to characterize tumor cells. The present research is to find answers to the following two questions: 1) Are the intracellular electrical potential and the transmembrane electrical resistance in tumor cells different from those in the normal cells? 2) Do the surface interacting agents such as Con A and polylysine, exert a different degree of effect on the uptake of amino acids in tumor cells and their normal counterparts?

CHAPTER II

METHODS AND MATERIALS

Chemical Induction of Skin Tumor

Six week old male or female C3H/F/He strain mice, weighing from 16 to 18 grams, were obtained from Texas Inbred Mice Company, Houston, Texas. The carcinogen solution was prepared by adding 3-methylcholanthrene (from Eastman Organic, Rochester, N.Y.) into thiophene free benzene until it reached the saturation point (about 1.67%). The frontal third of the back of the animals were shaved with a hair clipper a week before the first application of carcinogen. Only one drop of the carcinogen solution was applied at a time onto the interscapular area of the animal. This was repeated twice a week and continued for four weeks. In six animals a tumor developed within five weeks, in two mice it took about two months, and in one mouse the tumor was visually identifiable only after three months. Thus a tumor developed in all of the nine mice treated with 3-methylcholanthrene.

The animals were sacrificed for electrical measurements when the tumor size reached about 3mm x 5mm. Part of the tumor tissue was fixed in 10% formalin and reserved for histopathological studies. Slides with hematoxylin and eosin stain were prepared.

Transplantation of Tumor

A/J mice bearing solid subcutaneous tumors (type 15091A) were obtained from the University of Iowa as well as from the Jackson Laboratory, Bar Harbor, Maine. The tumor was maintained by subsequent transplantations into the host A/J mice. The following procedure of transplantation was adopted: the tumor tissue was removed and minced in a Petri dish with a pair of sharp scissors. The fine pieces of the tissue were loaded in a 17 gauge spinal needle. The loaded needle was then inserted just under the skin of the hind leg of the host mouse and the plunger stylus was pushed all the way to transfer the tumor tissues into the animal subcutaneously. This particular type of tumor grew very rapidly. Within a week the tumor mass reached the size of a marble.

In order to make a histological study, a small piece of the tumor tissue was fixed in 10% formalin, and slides with hematoxylin and eosin stain were prepared.

Tissue Culture

Only the cells of tumor type 15091A were grown in tissue culture medium.

Medium

The commonly used relatively simple Minimum Essential Medium (MEM) was proven to be an inadequate culture medium for the present line of cells despite the vast modifications in the sources of serums (calf, fetal calf and horse serum). Changes in the level of serum concentration in the medium also did not yield sufficient growth of the cells. Therefore, other ingredients were added in the "medium" and a number of combinations were

tested. Finally, a culture medium, so called medium B_1D, was established. This medium was used successfully in maintaining the cell lines under investigation. The same medium was used to initiate the growth of the primary explants derived from the subcutaneous tissue of the normal mice and was found to be adequate to maintain the subsequent cultures, although with a slow growth rate. Its composition is given in Table 1. The osmolarity of the medium B_1D was 300 mOsm as determined by a freezing point depression type osmometer. The pH of the medium ranged from 7.0 to 7.6 and was adjusted by bubbling 5% CO_2 and 95% air through it using phenol red as the indicator.

Solutions

Compositions of various solutions used in this study are listed in Table 2.

Methods of Tissue Culture

The cultures of both anaplastic tumor and normal subcutaneous tissue were initiated as primary cultures by explanation of some tissue without prior dispersion. The procedure was as follows: tissue was removed aseptically from the animal in front of a Westinghouse Clean Work Station Type WT. After rinsed rapidly in medium B_1D, the tissue was cut into small pieces and transferred into the T-25 plastic flask (Falcon Plastics). The pH of the medium was adjusted to 7.0 by bubbling with the gas mixture containing 5% CO_2 and 95% air. With anaplastic tumor cells the secondary and subsequent cultures were started simply by mixing 1.5 ml fresh medium with 1.5 ml of the suspending medium of the close to confluent culture flasks. However, with normal fibroblast culture there

TABLE 1

COMPOSITION OF THE MEDIUM B_1D

Component	Amount
Auto-Pow (Autoclavable Powdered MEM, Flow Laboratory, Rockville, Maryland)	6.56 gm/L
Dextrose	1.00 gm/L
Asparagine	1.60 mg/L
$CaCl_2$	80.00 mg/L
Phenol red	32.00 mg/L
Glutamine	2.00 mmole/L
NCTC 135(1x)	100.00 ml/L
Penicillin	100,000 units/L
Streptomycin	100,000 µg/L
Fungizone	2,000 µg/L
Fetal calf serum	200 ml/L
$NaHCO_3$	1.79 gm/L

TABLE 2

COMPOSITIONS OF VARIOUS SOLUTIONS

	Component	mM	Mg/L
"Mouse" Ringer's solution (94)	$MgCl_2$	1.0	
	$CaCl_2$	2.0	
	$KHCO_3$	5.0	
	$NaHCO_3$	7.0	
	NaH_2PO_4	1.0	
	NaCl	141.8	
	Glucose	11.0	
Na Ringer's solution	NaCl	115.0	
	$KHCO_3$	2.5	
	$CaCl_2$	1.5	
K Ringer's solution	KCl	115.0	
	$KHCO_3$	2.5	
	$CaCl_2$	1.5	
Normal saline	NaCl		9000.0
Dulbecco's phosphate buffered saline (PBS) (95)	NaCl	137.0	
	KCl	2.6	
	Na_2HPO_4	8.0	
	KH_2PO_4	1.5	
	$CaCl_2$	1.3	
	$MgCl_2 \cdot 6H_2O$	0.5	
Hanks balanced salt solution (BSS) (96)	NaCl	136.8	
	KCl	5.4	
	$Na_2HPO_4 \cdot 2H_2O$	0.4	
	KH_2PO_4	0.5	
	$MgSO_4 \cdot 7H_2O$	0.8	
	$CaCl_2$ (anhyd.)	1.3	
	Glucose	5.5	
	$NaHCO_3$	4.2	
	Phenol red		10.0
Calcium and magnesium free phosphate buffered saline (CMF-PBS) (97)	NaCl	136.8	
	KCl	4.0	
	Na_2HPO_4	0.5	
	KH_2PO_4	0.1	
	Glucose	11.1	
Trypsin solution (0.05%)	Trypsin		500.0 (dissolved in CMF-PBS)

was not enough mitotic cells in the medium to start new culture with adequate proliferation rate. Therefore, subculturing of normal cells was accomplished by treatment of trypsin. This was done by the following procedures: the medium in the culture flask was discarded and the cells were washed with BSS 1x for 3 min; 3 ml of 0.05% trypsin solution was added in the flask. The cells were immediately irrigated forcefully by the help of a Pasteur pipet and a rubber ball. The purpose of the irrigation is to detach the cells from the substratum. The trypsinization process was completed within 5 min. The subculture was initiated by adding 1 ml of trypsin solution with detached cells into each flask which contained 2.0 ml of fresh medium. The pH of the subcultured medium was adjusted to 7.0 as described previously. Approximately 12 hrs later, the trypsin-containing medium was replaced with fresh medium. In general the culture medium was renewed every four days. When the cell growth reached confluency, more frequent renewing of medium became necessary.

The growth of cells in culture was assessed by successive daily harvesting of a series of flasks which were subcultured at the same time with about the same number of cells. Growth curves were established by plotting protein contents of culture flasks against the length of the period of culture in days.

Microelectrodes

Preparation

The Kimax glass capillaries with outside diameter of 1.2-1.5mm and wall thickness of 0.2mm were cut in 6 inch pieces. They were cleaned in boiling distilled water for half an hour then dried in an oven. The clean, dry glass capillaries were then ready for the fabrication of

microelectrodes.

The microelectrodes used in this study were fabricated with a Chowdhury Pipette-Puller (98). Clean, dry glass capillary tubing is clamped to the tracks with the tracks in their most proximal position. The position of the heating coil is adjusted so that the glass capillary runs along the center of the coil. An initial tension of about four ounces is then applied to the steel wires at the solenoid by the adjustable mechanical spring, and the filament current turned on. As the glass gradually softens over a period of 5 to 15 sec, it gets evenly extended by the tension of the mechanical spring. When about 2 mm elongation of the softened portion of the glass capillary has occurred, as governed by the side arm of the track, contacts of the microswitch close, thereby energizing the solenoid magnet through a power relay. The magnet thus exerts the sudden final pull on the capillary tubing. At the same time heating current is turned off and with about a 4msec delay air jets are blown on to the softened portion of the glass tube. Thus the capillary is drawn to a fine point without excessive elongation of the tip region. Two micropipettes identical in shape and tip size are produced.

Microelectrodes fabricated with this technique have the advantage of higher mechanical rigidity, finer tip and lower tip resistance than conventional microelectrodes (98). The size of the tip had been reported less than 500Å as compared to the conventional microelectrodes which are usually about 0.5 μ. Therefore, the common problem of tissue distortion prior to the actual penetration was largely minimized. In fact, in several cases penetrations were performed repeatedly on the same cell without any sign of damaging the cell.

Filling Microelectrodes

Microelectrodes were filled with a solution of 1 M NaCl and 1 mM $CaCl_2$ instead of the commonly used 3 M KCl solution. This avoids the large tip potentials exhibited in KCl filled microelectrodes. Chowdhury (99) proposed that the negatively charged silicate ions fixed on the inner wall of the tip exert an electrical field upon the ions within the tip. Thus in the case of KCl filled microelectrodes, the chloride ions are restrained from diffusing outward while potassium ions are enhanced. As a result of this separation of charges a tip potential is generated in the electrode, the interior being negative with reference to the outside bathing solution. The reduction in the tip potential of the microelectrodes by filling them with NaCl and $CaCl_2$ was partially due to the relatively lower mobility of sodium ion than the chloride ion, and partially due to the neutralization of the negative surface charge by calcium ions.

Due to the fineness of the tip, the conventional techniques of filling of microelectrodes, such as alternate boiling and cooling, were not satisfactory in our case. The technique used here was a slight modification of that used by Byzov and Chernyshov (100), and by Chowdhury (98). This is as follows:

1. The tip of the microelectrode was immersed in the electrolyte solution (1M NaCl and 1 mM $CaCl_2$) in a tall beaker.

2. A drop of distilled water was placed in the open wide end of the microelectrode, and the beaker was placed inside a dessicator with a small amount of distilled water in it. Within 24 hrs, the tip became wet by the vapor and this wetting helped the electrolyte solution to climb

up in the tip and thus fill the very end of the tip.

3. The beaker was then filled with the electrolyte solution to cover the whole micropipette and placed in a vacuum oven under reduced pressure and at a temperature of 65°C. Most of the micropipettes became filled with the electrolyte at this stage.

4. After half an hour, the temperature and pressure of the oven was brought back to the ambient levels. Small air bubbles occasionally trapped within the electrode were removed by a very fine stainless steel wire.

Variations of Tip Potential Change with Ionic Concentrations and Compositions

The tip potential and resistance of the microelectrodes were checked before using for cell punctures. It is known that the intracellular electrolyte composition is quite different from the extracellular environment; the former has high potassium and low sodium ions whereas the latter has low potassium and high sodium ions. Therefore, it can be expected that the tip potential of a microelectrode placed within a cell would be different from that when the microelectrode is in the extracellular fluid or bathing fluid. Consequently, the potential of a number of microelectrodes was first measured in K-Ringer's solution and then in Na-Ringer's solution.

Electrical Recording Systems

The microelectrode, held by a micromanipulator, was connected to the input of an electrometer (Model M4A, W. P. Instruments) via a salt bridge and a calomel half cell. Similar arrangement was used for the indifferent electrode except it was connected to the ground point of the

electrometer. The output of the electrometer was connected to the Low-level DC Preamplifier and the recording system of a Grass Polygraph. The input impedence of the electrometer was 10^{12} ohms. Besides the traditional potential measurement, this electrometer was also equipped with a built-in circuit which permits direct measurement of resistance. This is done by injecting current pulses through the microelectrodes and monitoring the voltage drop across the termini of the electrometer. The overall recording system is illustrated in a block diagram in Figure 1.

Electrical Measurements

Electrical Measurements of Skin Tissue

A segment of skin of normal or tumorous C3H mouse was firmly held against a lucite chamber base by a wide-eyed nylon net. The whole chamber was mounted on the stage of microscope and the microelectrode penetration was performed under observation with the help of a dissecting microscope. Mouse Ringer's solution was kept circulating in and out of the lucite chamber, so that the tissue was always bathed in fresh solution.

Electrical Measurements of Tissue Culture Cells

The roof of the plastic culture flask was removed partially to allow the entry of microelectrode. The flask was then fixed on the stage of a Nikon inverted phase contrast microscope. Under 640x magnification, the microelectrode with a 90° bend near the tip was maneuvered close to the cell to be impaled with the axis of the microelectrode tip almost vertical to the cell. The finer advancement of the microelectrode was then achieved with the aid of a motor driven micromanipulator. This set-up enabled a smooth, slow movement of the microelectrode at a rate of

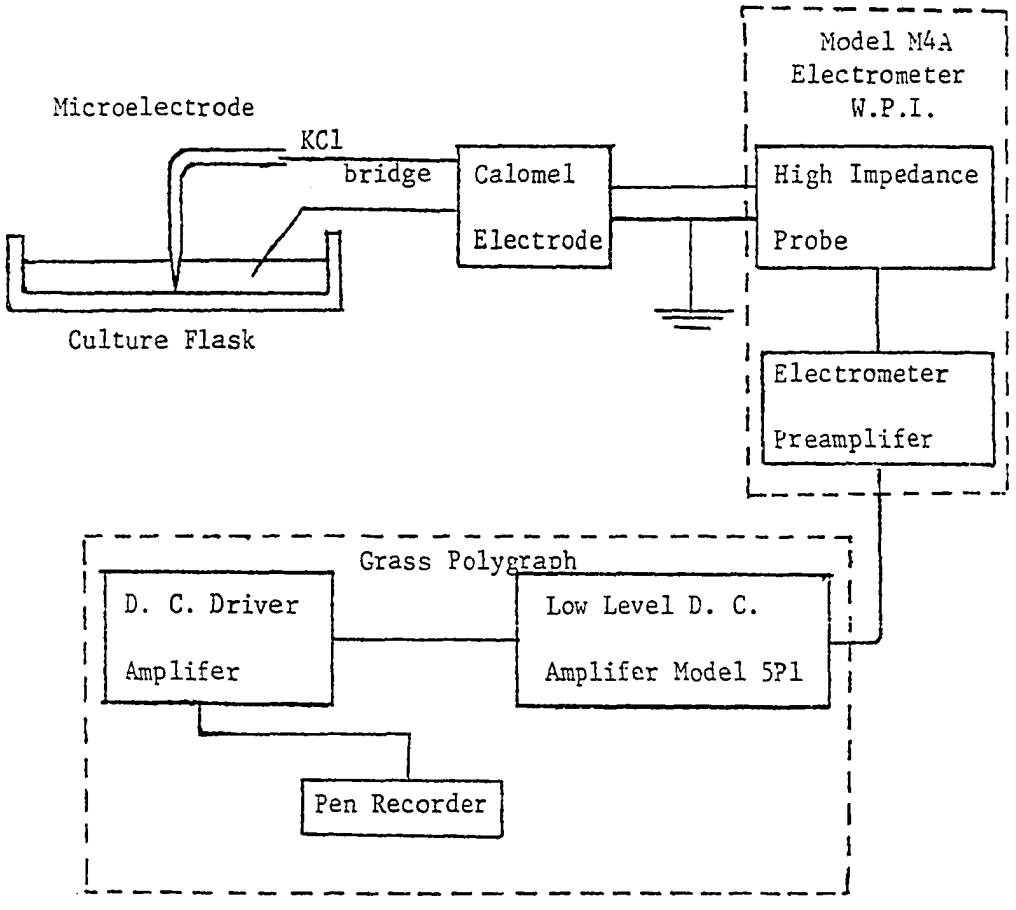

Figure 1. Block diagram of recording apparatus for electrical measurement.

12.5 μ/min. At the instant the tip penetrated the cell membrane a sudden change in potential was monitored and the motor was then turned off. In most cases the microelectrode remained inside the cell for at least three minutes and was then withdrawn. Withdrawal of microelectrode was also achieved by the motor driven micromanipulator.

Amino Acid Uptake Studies

Only the tissue culture cells of the transplantable tumor and normal fibroblasts from the subcutaneous tissue of homologous mouse were investigated for the uptake of amino acids. Both types of cells were grown essentially as monolayer in culture flask.

Protein Determination

The uptake of amino acids was expressed in the units of picomoles per μg of cellular protein. Lowry's method was adapted for protein determination (101). The Folin's phenol reagent contains mainly phosphomolybdic and phosphotungstic acids. Both acids are readily reduced in alkaline condition by phenol or oxybenzol compounds, yielding a blue color. Proteins generally contain aromatic amino acids such as tyrosine and tryptophan, and thus are able to reduce the Folin's phenol reagent forming color products. It was found that better results were achieved in the presence of sodium carbonate and copper sulfate in the mixture of reagents. The Na_2CO_3 increases the stability of the color product whereas $CuSO_4$ enhances the intensity of color reaction and accelerates the color development.

Scanning of Amino Acid Uptake Studied With an Amino Acid Analyzer

Since no information is available about the amino acid uptake by

this particular tumor in tissue culture, the following questions needed to be answered: Are these in vitro tumor cells capable of concentrating amino acids at all? If so, which amino acids are taken up predominantly?

Experiments were designed with an attempt to answer these questions. Cells were exposed to high concentration of amino acids mixture for a certain period of time and then lysed in 0.1M NaOH. The amino acids composition in the lysate was analysed by Beckman Model 120C Amino Acid Analyzer. The area under each peak was calculated by the Model CRS-110A Infotronics Automatic Digital Integrator. In the control set cells were bathed in the regular medium before lysis by NaOH, and the same analysis of amino acid composition was performed. Since the present tumor cells are not sensitive to the hyperosmotic environment, the experimental incubation medium was prepared simply by adding 10 mM of each of four to six amino acids into the medium B_1D. Three experiments were performed using three different combinations of amino acids, e.g., aspartic acid, glutamine, glycine, alanine, and leucine in the first experiment; threonine, serine, glycine, valine, methionine and phenylalanine in the second experiment; and lysine, histidine, tryptophan and arginine in the last one.

The exact procedure is outlined below:

Two T-25 flasks were used for both experimental and control sets in order to have adequate amount of cells. After washed by medium B_1D 5 ml twice, the cells were incubated at 37°C for 1 hr with amino acids-added medium 3 ml for the experimental set and with regular medium B_1D 3 ml for control set. At the end of the incubation period, the cells were washed rapidly by cold BSS 5 ml three times and normal saline once.

After the washing solution had been completely removed, 1.5 ml of 0.1 N NaOH was added in the first flask and shook well. The NaOH cellular lysate was then transferred into the second flask. After sonication for 2 min, 0.1 ml of the lysate was taken for protein determination by Lowry's method. The rest of the lysate was added with 0.15 ml, 55% TCA (trichloroacetic acid). After centrifugation, the supernatant was separated from the precipitant and injected into the Beckman amino acid analyzer.

Amino Acid Uptake Studied by Labelled Amino Acids

From the previous experiments, three amino acids which showed relatively higher uptake were selected for further study.

Tracer quantities of tritiated amino acids were added in the incubation medium. By knowing the specific activity of the radiolabelled amino acids in the medium and by determining the rate of entry of the radioactive amino acids into the cell, the uptake of the unlabelled amino acids was calculated. In all these calculations the outflux of radioactive amino acid back into the medium was neglected.

The general procedure for isotope study is described as follows: Tissue culture cells within the T-25 flask were washed by BSS 1 x twice, then they were incubated with 3 ml hot amino acid added medium B_1D at 37°C for 1 hour. At the end of incubation, the medium was collected for checking the specific activity. The cells were then washed with ice cold normal saline 5 times within 1 min. 1.5 ml 0.1 N NaOH was added in each culture flask to lyse the cells. The cellular lysate underwent ultrasonication for 2 min. 0.2 ml of the lysate was used for protein determination by Lowry 's method, and another 0.2 ml was added into 6.0 ml scintillation fluid for isotope counting. The uptake was calculated in terms of

picomole per µg protein. The process of calculation was outlined in the following sequence:

$$\text{CPM (count per minute)} \rightarrow \text{CPM/µg protein} \rightarrow \frac{\text{CPM/µg protein}}{\text{specific activity (CPM/µmole)}}$$

$$\text{µ mole/µg protein} \rightarrow \text{picomole/µg protein}$$

Study I - Effects of Concentrations of Amino Acid in the Incubation Media on Amino Acid Uptake

A set of flasks which were subcultured on the same day with about the same number of cells were used. The same radioactive incubation medium was used repeatedly, and the increase of concentration was achieved by successive addition of the right amount of amino acid in the incubation medium. The procedure for this study was the same as listed in the previous section. The highest concentration used was 80 mM.

Study II - Effects of Concanavalin A (Con A) on Amino Acid Uptake

Grade III, highly purified Con A was obtained from Sigma Chemical Company. It contains approximately 15% protein, 85% NaCl and is substantially free of carbohydrates. Double crystallized, salt free trypsin, and trypsin inhibitor extracted from soybeans were also purchased from Sigma Chemical Company.

The monovalent Con A solution was prepared according to that described by Burger and Noonan (41). For making 30 mg of Con A solution 200 mg of Con A powder (containing approximately 30 mg Con A) was dissolved in 30 mg of Dulbecco's PBS. After the solution had been treated with 30 mg of trypsin for 5 hours at 37°C, 30 mg of soybean trypsin inhibitor was added to stop the enzymatic reaction. After sterilization by filtration through 0.2µ filter unit, the Con A solution is ready for use.

Subcultures cultivated at the same time and started with approximately the same number of cells were used for these studies. The general procedure for labelled amino acid study was adapted with the exception that preincubation was required before the cells were bathed in the hot transporting medium. After the flasks were washed twice with BSS 1x, the cells were incubated with various Con A solutions at 37°C for one hour prior to the incubation in radioactive transporting medium. After completion of preincubation, the cells were washed three times with 40 seconds by cold normal saline. The radioactive transporting medium of these studies contained 20 mM of either glycine, phenylalanine or histidine and the specific activity was made approximating 0.3 mCi/m mole.

Study III - Effects of Polylysine on Amino Acid Uptake

The methods were exactly the same as in Study II, with the exception that preincubation period was 10 min instead of 1 hour and in the pre-incubation medium polylysine was dissolved in medium B_1D with concentrations ranging from 50 to 200 mg/ml.

Study IV - Effects of Dinitrophenol (DNP) and Iodoacetate on Amino Acid Uptake

The procedure described above in Study II was followed here, but instead of preincubation, DNP and/or iodoacetate were dissolved in the hot transporting medium.

Study V - Effects of Temperature on Amino Acid Uptake

The method described in the general procedure was also applied to this study, except that the temperatures of incubation were varied. Uptake of amino acids was studied at 27°C, 32°C and 35°C respectively. The radioactive transporting medium contained 20 mM of the amino acid studied,

and the specific activity of the medium was 0.3 mCi/m mole.

Study VI - Effects of α-Methyl-D-glucopyranoside (αMG) on Concanavalin A Inhibition of Amino Acid Uptake

Same method as described in Study II was applied. The only difference was that 0.1 M αMG was present in the Con A preincubation solution.

Statistical Analysis

The majority of experimental results in this investigation were considered upon either the comparison of experimental and control groups or the comparison of some parameters measured in malignant and normal cells. Student's t test (102) was applied for the analysis of the statistical significance of the difference between results obtained from the two groups in comparison. A probability of less than 10% was regarded significant. In some results the linear correlation was expressed by the plot of a regression line, and the degree of linearity was determined by the correlation coefficient (103). When the correlation is perfect, the correlation coefficient equals to 1. The actual calculations were performed on a computerized Olivetti 101 Calculator.

CHAPTER III

RESULTS

Histological Study of Chemically Induced Skin-Tumor

The microscopic features of the skin tumor are shown in Figure 2 and Figure 3. In Figure 2, extensive invasion of epidermal cells into the dermis is observed. The neoplastic cells show dyskeratosis, hyperchromasia and different degrees of differentiation. In Figure 3, the neoplasm is rather restricted in epidermis; however, hyperkeratosis, parakeratosis and marked acanthosis are observed. Under high power, disorder of cellular polarity in epidermis is noted. The diagnosis of this skin disorder is squamous cell carcinoma.

Histological Study of Transplantable Tumor

As shown in Figure 4a and 4b, the highly destructive undifferentiated cells invade and destroy the muscle layer. Under high magnification, the cell shows irregularity in size and morphology. The nucleus: cytoplasm ratio is generally increased and hyperchromatic bizarre nuclei are found in high proportion. This transplantable tumor is diagnosed as undifferentiated carcinoma (anaplastic carcinoma).

Tissue Culture Cells Observed Under Phase Contrast Microscope

The transplantable tumor cells in tissue culture observed under

Figure 2a. Histology of chemically induced-skin tumor (I). Irregular masses of epidermal cells proliferate downward from the surface epidermis and invade the dermis. The neoplastic cells vary in the level of differentiation, ranging from differentiated and keratinized cells to anaplastic squamous cells.

Figure 2b. High-magnification of Figure 2a. Note a group of anaplastic squamous cells invading the dermis. These cells show dyskeratosis and hyperchromasia of nuclei.

Fig 2a

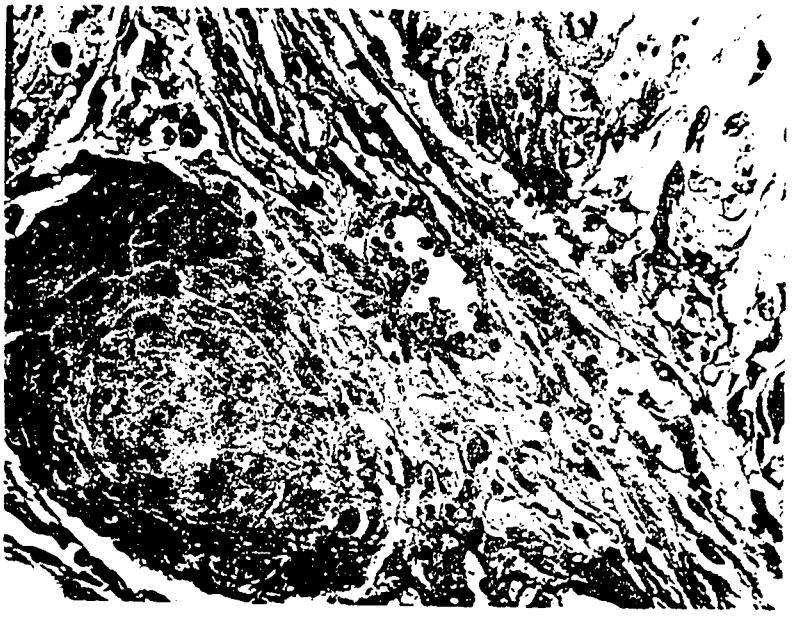

Fig 2b

Figure 3a. Histology of chemically induced-skin tumor (II). The skin demonstrates hyperkeratosis, parakeratosis and marked acanthosis. There is no evidence of dermal invasion.

Figure 3b. High-magnification of Figure 3a. The picture shows the disturbance of cellular maturity and polarity in epidermis. However, these cells are uniform and have no abnormal mitosis.

Fig 3a

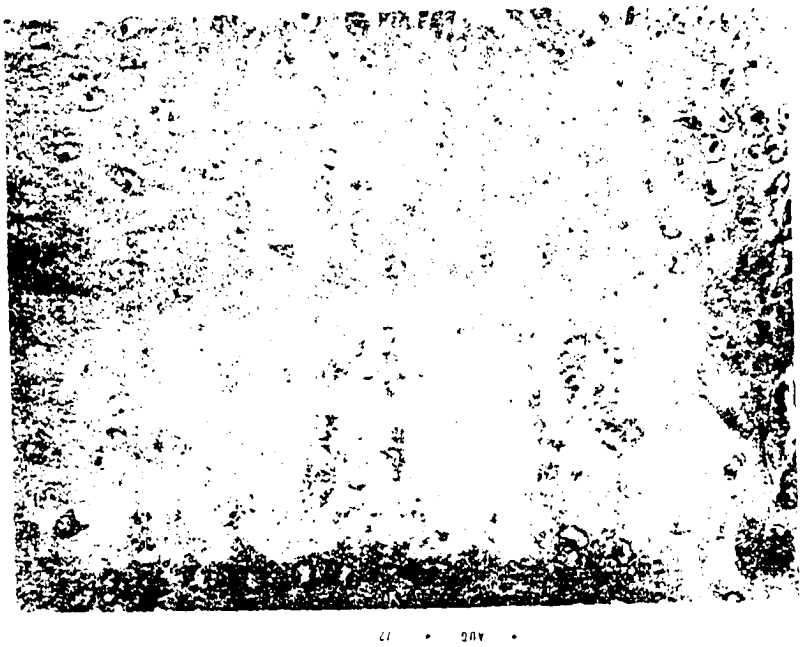

Fig 3b

Figure 4a. Histology of transplantable mouse tumor. The picture shows highly destructive undifferentiated cell carcinoma transplanted into the subcutaneous tissue of mice. The muscle is largely destroyed by diffuse proliferation and invasion of the neoplastic cells.

Figure 4b. High-magnification of Figure 4a. Note that the cells are very irregular in shape and size, having hyperchromatic bizarre nuclei with clumped chromatin.

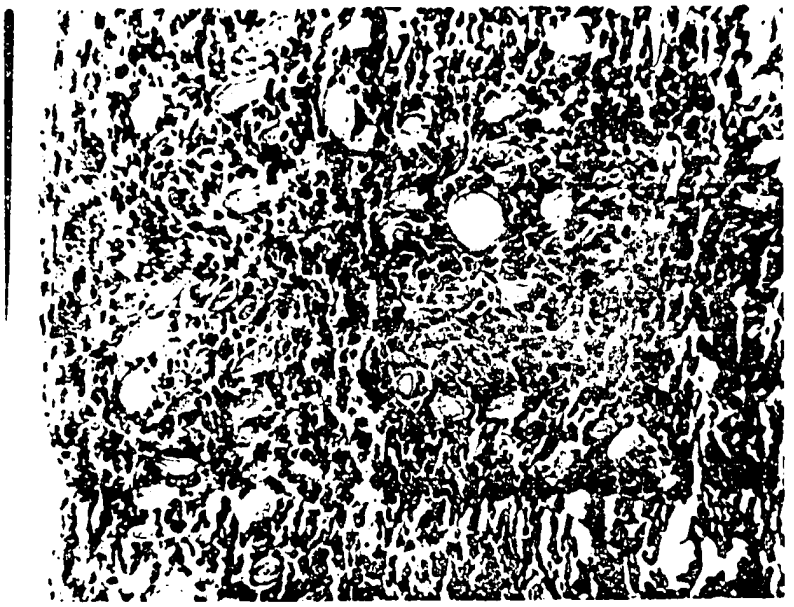

Fig 4a

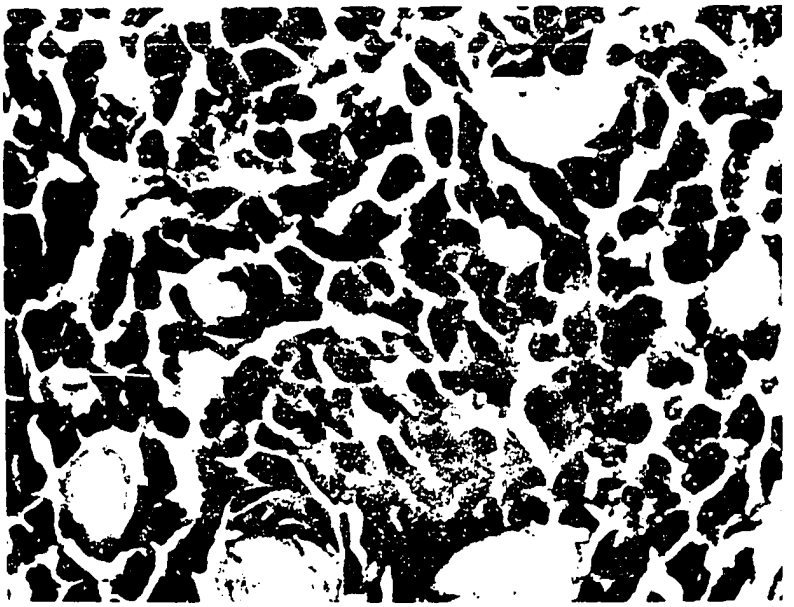

Fig 4b

a phase contrast microscope are shown in Figure 5. The cells are quite irregular in shape because of the development of pseudopodium-like projections which are associated with their movement on the substratum. However, generally they show an ellipsoid shape with two, three or even four cytoplasmic projections. A single cell may have either one or two nuclei with multiple nucleoli. The cytoplasm is richly granulated. The cells are anchored onto the surface of the bottom of the flask and form primarily a monolayer with an occasional overlapping of the cytoplasmic projections. Cells undergoing mitosis are rounded up and some of them float in the medium.

Because of the high degree of irregularity in the shape of the cancer cells in a tissue culture, it is rather difficult to determine the volume of these cells. However, when treated with trypsin, the cells get released from the substratum and they become quite uniformly spherical in shape. An advantage of this fact was taken in the calculation of the volume of cancer cells. The diameter of the trypsinized cells was measured with the aid of an ocular micrometer. The diameter estimated from 50 measurements of randomly chosen cells was 17.10 ± 0.2 μ. The mean cell volume was therefore calculated to be 2.6×10^{-9} ml.

The morphology of cultured normal fibroblasts derived from the subcutaneous tissue of normal A/J mouse is shown in Figure 6. The spindle-shaped cell is thinner and longer than the corresponding tumor cell. Cells with single nucleus and two nucleoli are most often seen. Groups of fibroblasts have a tendency to form parallel bundles interweaving with each other at small angles as the arrangement of muscle fibers.

It has been verified in our laboratory as well as in other

Figure 5a. The transplantable anaplastic carcinoma cells in tissue culture observed under a phase contrast microscope (320x). The finest division of the scale represents 5μ of length. See text for description.

Figure 5b. High magnification of Figure 5a (640x). The finest division of the scale represents 2.5μ of length.

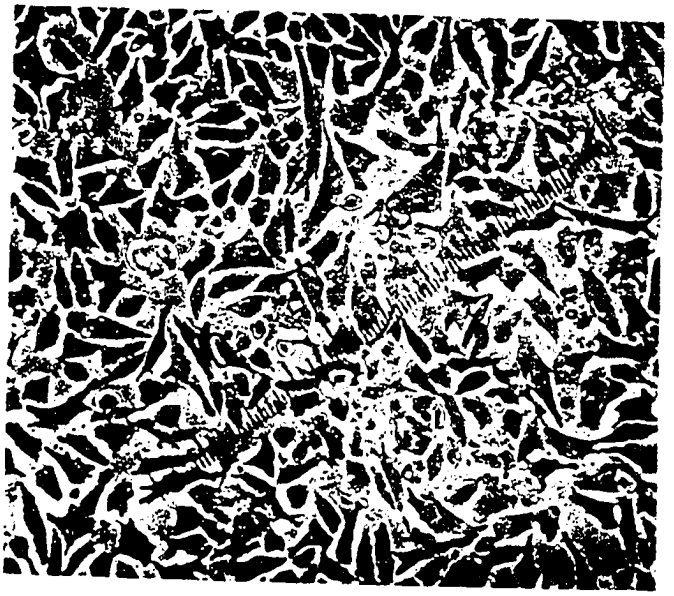

Fig 5a

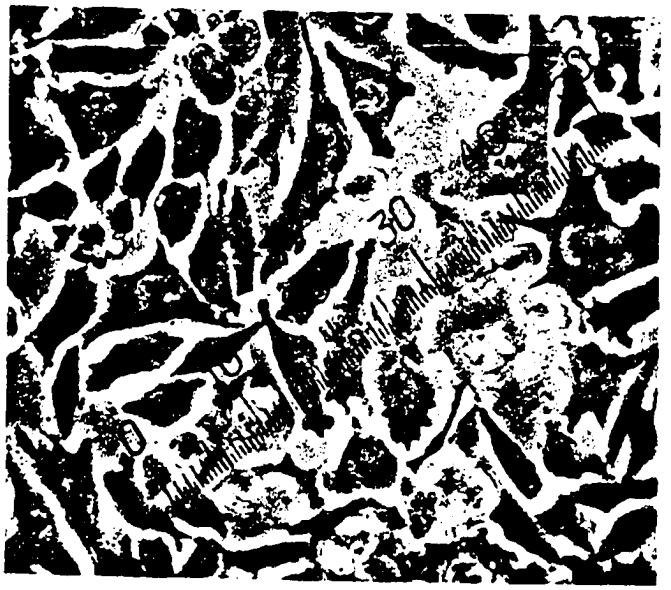

Fig 5b

Figure 6a. The cultured fibroblasts from subcutaneous tissue of normal A/J mouse observed under a phase contrast microscope (320x). The finest division of the scale represents 5μ of length. See text for description.

Figure 6b. High-magnification of Figure 6a (640x). The finest division of the scale represents 2.5μ of length.

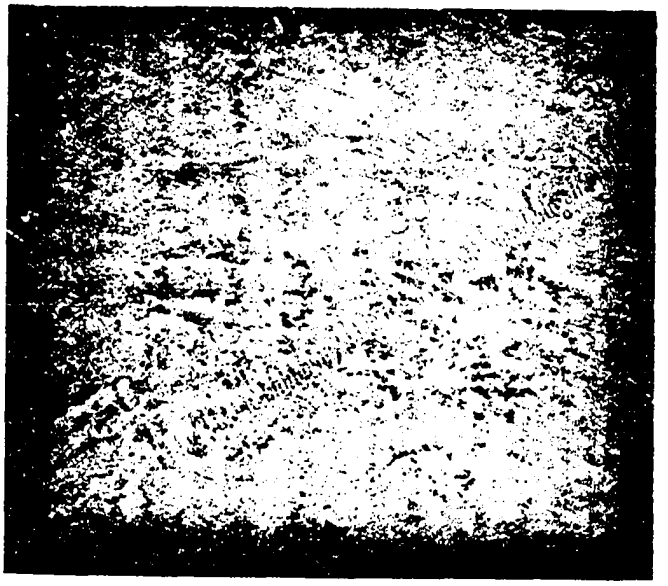

Fig 6a

Fig 6b

laboratories (38) that the amount of protein in any colony of cultured cells is directly proportional to the number of cells present in that colony. Based on the linearity observed between protein content and cell number, the growth rate of the cultured cells was determined by chronological follow-up of the increase in protein content rather than the number of cells in a series of simultaneously subcultured flasks. The reason for choosing protein content to determine growth is that protein determination is much more accurate than cell counting. In the preparation for cell counting, some cells are damaged or completely lysed by the trypsin treatment and its associated mechanical irrigation, and therefore the accurate assessment is difficult without a larger number of experiments. On the contrary, the determination of protein content does not involve these difficulties. The growth curve is therefore plotted as protein content against the period of culture (in days) in a semilogarithmic graph as shown in Figure 7. Each point represents the average of 3 experiments. The doubling time obtained from this graph is 3.6 days.

Properties of Microelectrodes

The resistance of the microelectrodes ranges from 5 to 25 MΩ; the higher resistances correspond to microelectrodes with finer tips. The tip potentials of these microelectrodes are considerably lower than those filled with 3M KCl, and their values range between -14 mV and +8 mV with the majority of the microelectrodes having tip potential very close to zero.

Since the tip potential of a microelectrode varies with the ionic compositions and concentrations of the dipping solutions, it is necessary

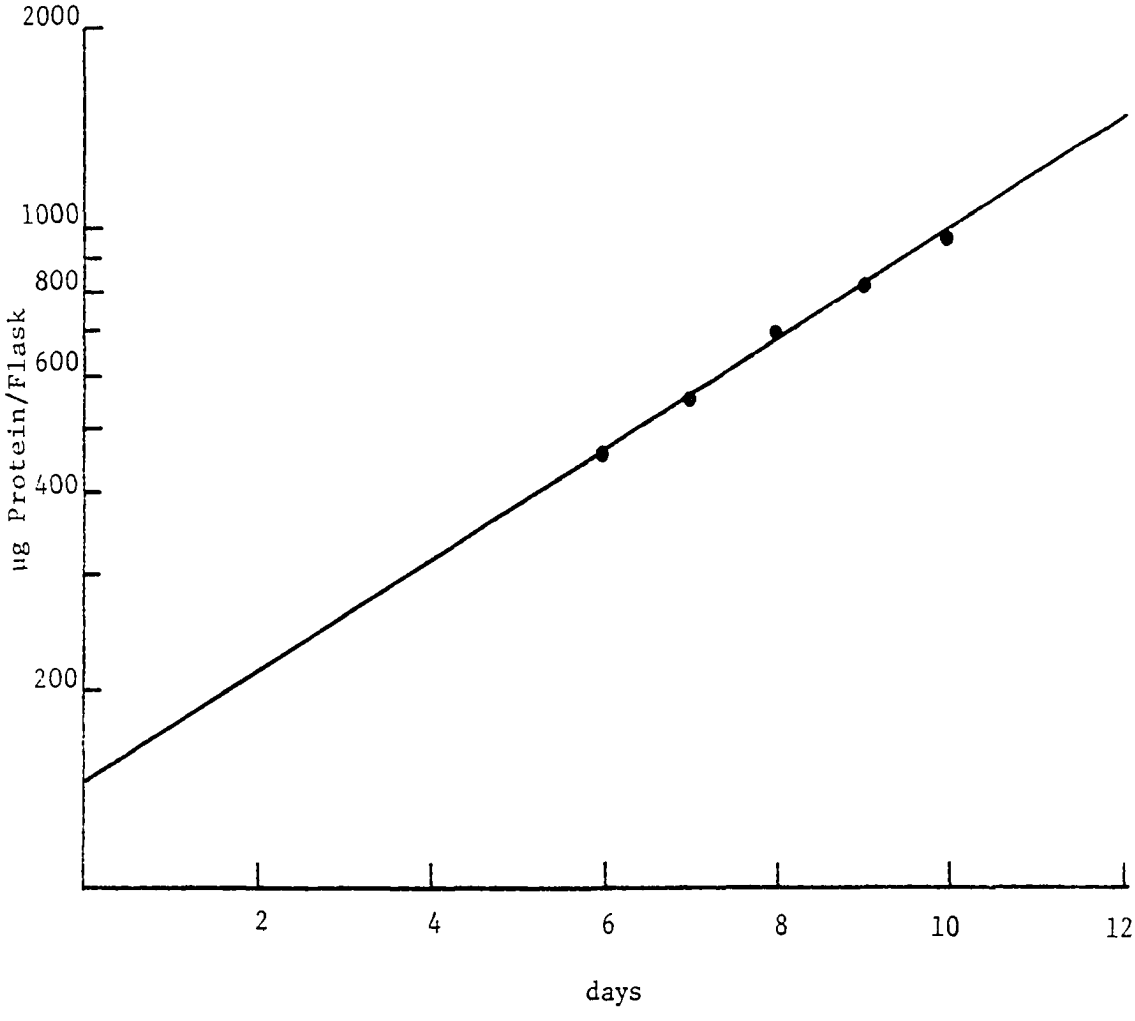

Figure 7. The growth curve of anaplastic carcinoma cells in tissue culture. Each point represents the average of three experiments. The doubling time obtained from this graph is 3.6 days.

to determine the exact magnitudes of such variations in the tip potential. The tip potentials of 22 different microelectrodes were detected first in K-Ringer's solution and then in Na-Ringer's solution. It was observed that microelectrodes with higher resistances and/or more negative tip potentials had larger magnitudes of changes in tip potential between the two test solutions. Figure 8 represents the plot of the change in the tip potential against the microelectrode resistance, whereas Figure 9 represents the plot of the change in tip potential against the intrinsic tip potential of the microelectrode in Na-Ringer's solution. The least square linear regression lines are indicated in the figures by the solid lines. The correlation coefficient of the parameters in Figure 8 is 0.64 whereas that in Figure 9 is 0.95.

Note that microelectrodes with low resistance and low intrinsic tip potential had hardly any change in their tip potential in going from K-Ringer's solution to Na-Ringer's solution. These microelectrodes warrant no correction of the measured bioelectric potential. With all other microelectrodes, however, corrections of the measured intracellular potential were made with the aid of the graph in Figure 9, especially since the linearity of this graph is extremely good.

Electrical Measurements in Intact Skin (C3H Strain of Mice)

Typical polygraph recordings of the electrical measurements are shown in Figure 10. Record (a) illustrates a successful puncture. A sharp change in intracellular potential was observed right after penetration. The potential was stable for more than 2 minutes without any detectable declination. Following the withdrawal of the microelectrode out of

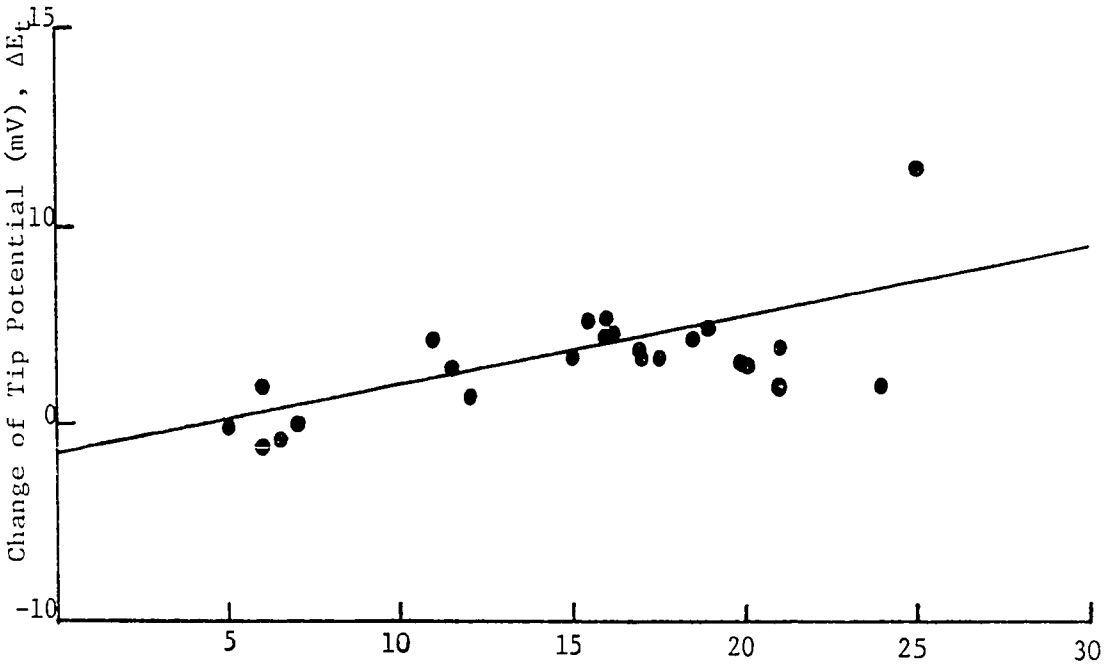

Figure 8. The relationship between resistance of microelectrode and magnitude of tip potential change caused by placing the microelectrode from K-Ringer's solution to Na-Ringer's solution. The solid line is the least square regression line. $\Delta E_t = (1.91 \pm 1.22) + (0.30 \pm 0.07)R$. The K-Ringer's solution simulates the intracellular fluid and the Na-Ringer's solution simulates the extracellular fluid or the bathing medium.

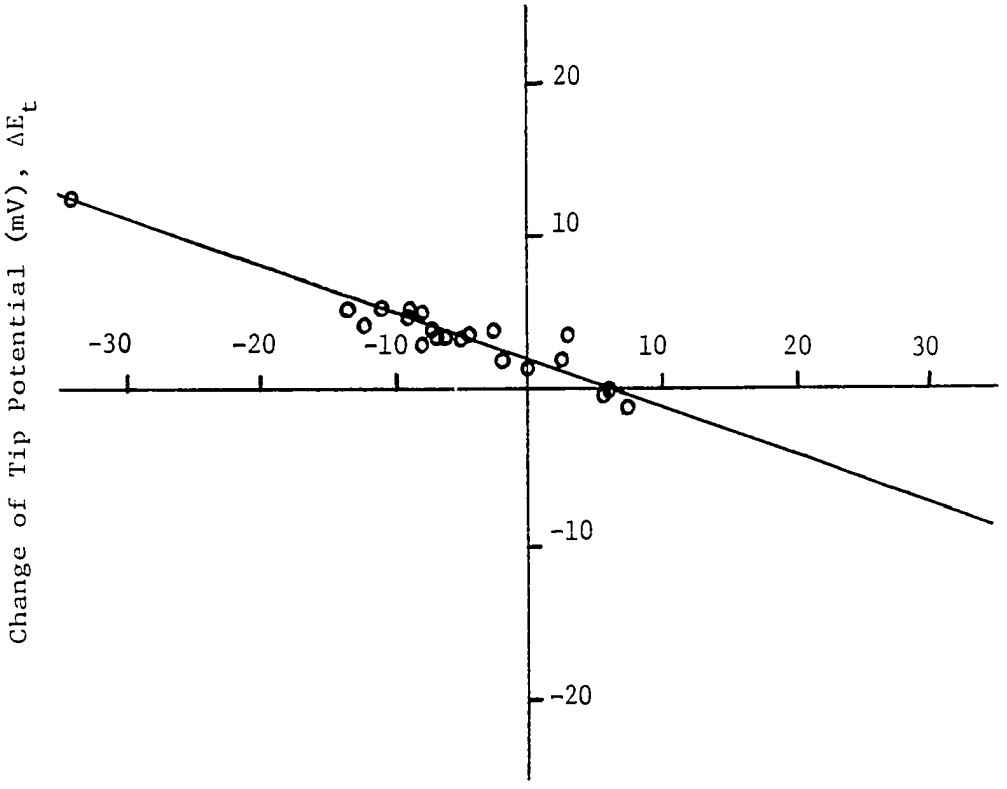

Figure 9. The relationship between intrinsic tip potential of microelectrode and magnitude of tip potential change caused by placing the microelectrode from K-Ringer's solution to Na-Ringer's solution. The solid line is the least square regression line. $\Delta E_t = (1.90 \pm 0.19) + (-0.30 \pm 0.02)E_t$. The K-Ringer's solution simulates the intracellular fluid and the Na-Ringer's solution simulates the extracellular fluid or the bathing medium.

Figure 10. Polygraph recordings of intracellular potential and membrane resistance of skin tumor cells in mouse Ringer's solution. Ordinate represents the potential (mV) and abscissa time (min). B denotes the baseline of the polygraph tracing. The negative potential is indicated by the downward shifting of the tracing (-7mV for recording a). P denotes the point of penetration of the microelectrode. At S the motor-driven advancement of the microelectrode is stopped. The complete withdrawal of the microelectrode is denoted by W. The intermittent vertical lines represent the magnitudes of voltage drops associated with pulses of constant current sent through the microelectrode for the resistance measurement. The intracellular potential and membrane resistance of the successful puncture are expressed in parenthesis.

Recording (a). A successful puncture; intracellular potential remains stable during the period the microelectrode is in the cell.

Recording (b). The cell is damaged by the impalement of microelectrode as revealed by the zero membrane resistance of the cell.

Recording (c). An unsuccessful puncture due to damage of the cell along with breakage of the tip of the microelectrode.

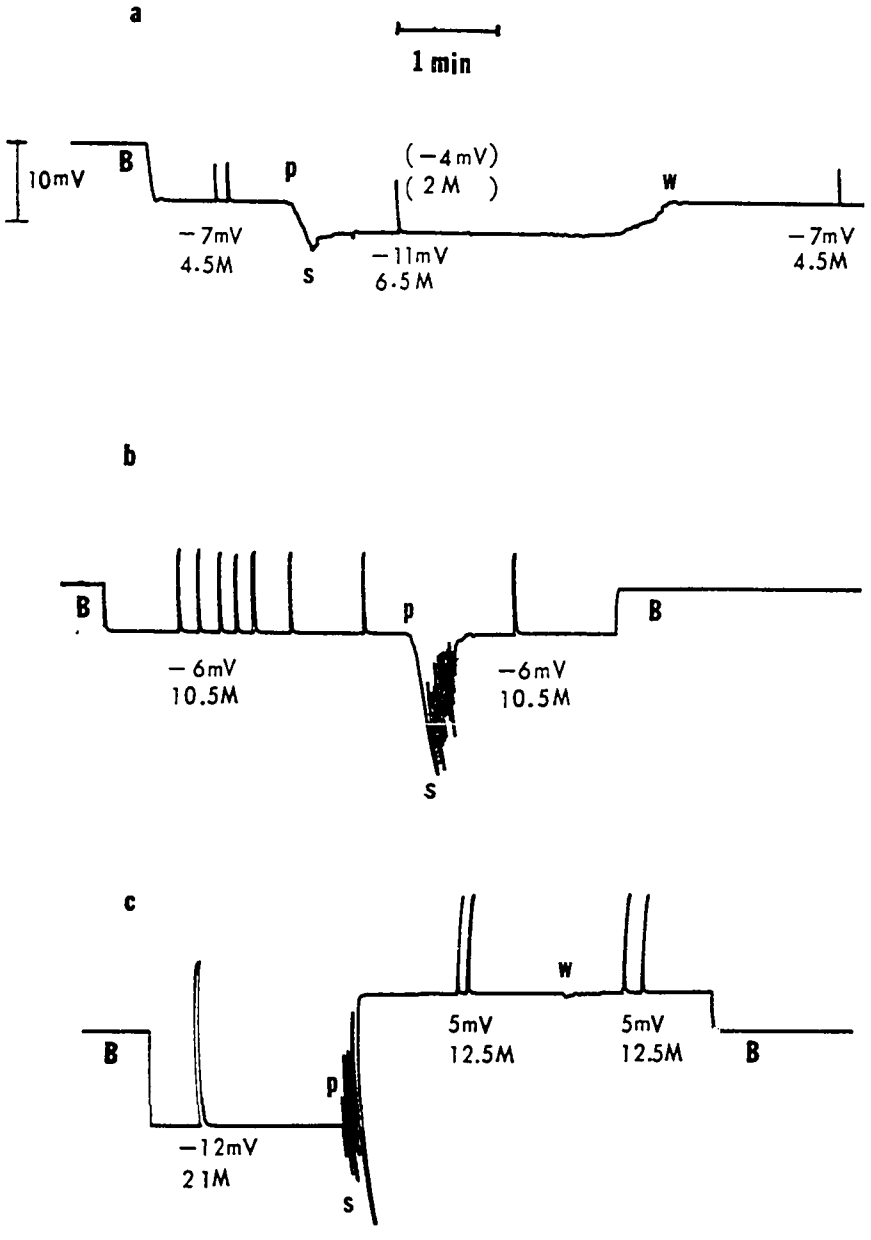
a
1 min
10mV
B
p
(−4mV)
(2M)
w
−7mV
4.5M
s
−11mV
6.5M
−7mV
4.5M
b
B
p
B
−6mV
10.5M
−6mV
10.5M
s
c
w
B
5mV
12.5M
5mV
12.5M
B
p
−12mV
21M
s

Figure 10.

the cell, the potential returned to the pre-penetration level. The resistance of the microelectrode was found to be the same before penetration and following the withdrawal from the cell, indicating that the tip is neither broken nor plugged with any organic substance.

In some instances, the tip potential and/or the resistance of the microelectrode following withdrawal from the cell were different from the respective values prior to penetration into the cell. In these cases, a decision was made to use the post-penetration values for calculation of intracellular potential and membrane resistance, the reason being that the chance of breaking or obstructing the tip of a microelectrode is much greater while inserting than when withdrawing out of the cell.

Record (b) illustrates the situation when the cell was damaged by the microelectrode. Following the initial jerk the potential fluctuated vigorously for a little while and then declined to the pre-penetration level, although the microelectrode was not withdrawn. The membrane resistance of the cell was very close to zero. Under the microscope the cell was found to form a big vacuole, undergo granulation and swelling and finally disintegrated. The microelectrode seems to be still intact, as judged from its tip potential and resistance.

Record (c) demonstrates an unsuccessful puncture due to damage of the cell along with breakage of the tip of the microelectrode. After a sudden and transient fluctuation, the potential changed to positive polarity and the resistance was markedly reduced despite the fact that the electrode was still inside the cell. Subsequent to withdrawal of the microelectrode, there was no further change on either the potential or resistance. This can be explained easily as the result of disruption of

the cytoplasmic membrane. The decrease of resistance of the microelectrode is an indication of a broken tip.

Figure 11 represents the data on the intracellular potentials in normal cells and induced tumor cells of the skin of mice (C3H strain). In normal, as well as in cancer cells, the intracellular potential is negative with respect to the reference electrode placed in the bathing solution. However, the magnitudes of the intracellular potential of the tumor cells are lower than those of the normal cells. In addition, the intracellular potential of the tumor cells varies widely between -5 and -32 mV, whereas the range of potentials of normal cells is limited within a narrow range of -25 and -34 mV. Even the average intracellular potential of the tumor cell is significantly different from that of the normal ones as reflected by Student's t test where $P<10^{-12}$.

The results of the measurements of membrane resistance are shown in Figure 12. Most of the tumor cells have a membrane resistance higher than the mean resistance of normal cells. The difference of resistance in normal and malignant cells is statistically highly significant ($P<10^{-8}$). The resistance of tumor cells also shows a wider spread in its magnitude than is the case in normal cells.

Electrical Measurements in Tissue Culture Cells A/J Strain of Mice

The intracellular potentials of anaplastic carcinoma cells and normal fibroblasts were both very low. The mean intracellular potential of cancer cells is -4.9 ± 0.4 mV and that of normal cells is -0.6 ± 0.5 mV. Extreme difficulty has been encountered in measuring the intracellular potential of the normal fibroblasts. The cells growing in medium B_1D

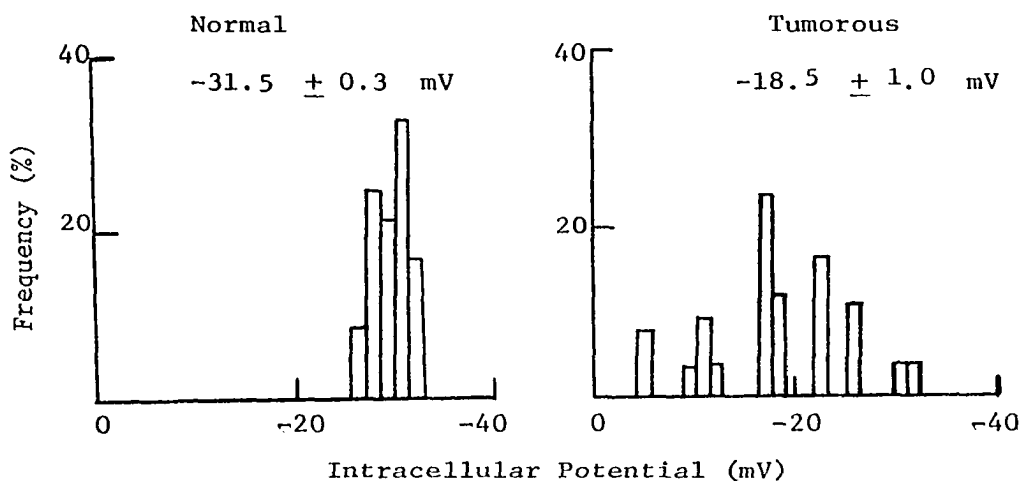

Figure 11. The intracellular potentials of normal and tumor cells of the skin of mice (C3H strain). The means and standard errors are shown at the top of the graph.

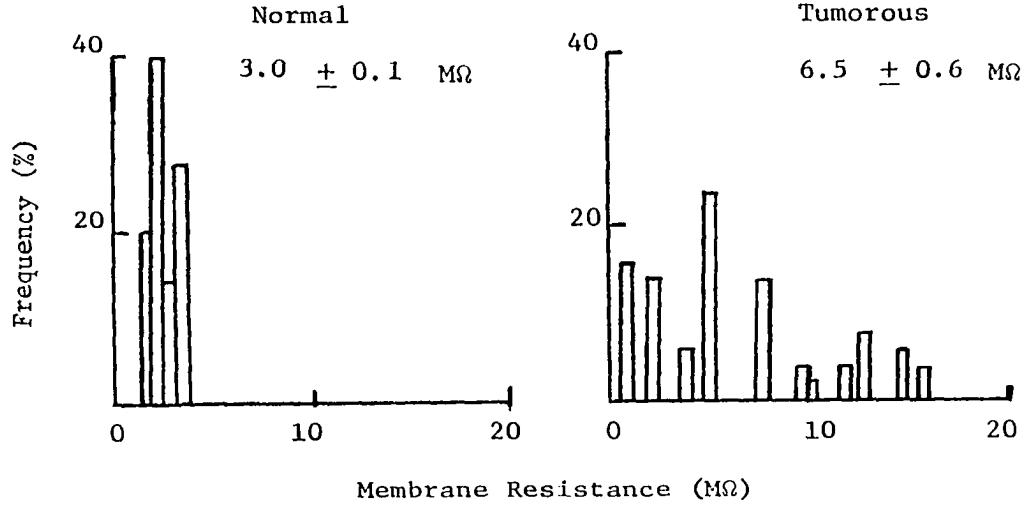

Figure 12. The membrane resistances of normal and tumor cells of the skin of mice (C3H strain). The means and standard errors are shown at the top of the graph.

are long but very thin in thickness (Figure 6a and 6b). Despite a tremendous effort, only 30 successful punctures were secured. The potentials ranged from -6 to +8 mV, with more than half punctures having potentials between -2 to +1 mV.

Thirty-one measurements with normal cells and 109 measurements with tumor cells indicate that there is no significant difference in the membrane resistance of carcinoma cells from their normal counterparts.

Scanning of Amino Acid Uptake Studied with an Amino Acid Analyzer

Since there is no report in the literature on the uptake of amino acids by the present types of cells, the first thing to do was to scan as many as fourteen amino acids to see which of them were predominantly taken up by the cells. The cellular concentration of amino acids is expressed in terms of picomole of amino acids per μg of cellular protein. The reason is that with cell-counting, cells have to be removed from the substratum by a trypsinization process which contradicts the experimental requirement of a monolayer of cells for the study of amino acid uptake. On the other hand, the protein determination can be achieved very accurately by a small amount of the lysate obtained after completion of the experiment. Since a linear relationship between protein content and cell number has been verified routinely, protein content was determined instead of cell counting.

The cellular amino acid contents were determined first when the cells were incubated in the normal growth medium and then when the cells were incubated in a growth medium which contained 10 mmole per liter extra concentrations of each of a group of four to six amino acids (denoted by

asterisks in Table 1). When the ratio of any amino acid concentration in the second incubating medium to that in the normal medium was found not to be significantly greater than one (as represented in the last column of Table 1), then that amino acid was discarded from being studied any further. It is argued that the transport of an amino acid can be studied effectively with the use of radioactive tracers only when the concentration ratio is significantly greater than one.

As shown in Table 3, with the exception of aspartic acid, glutamic acid, threonine, arginine and lysine, all the other nine amino acids studied have more than a 2.5-fold increase in their cellular concentration when the cells are incubated in the modified medium. Histidine and tryptophan have the concentration increased more than 10 fold. Alanine, serine and phenylalanine have a 5 to 7 fold increment. The concentrations of glycine, leucine, methionine, and valine are increased from 2.5 to 4 fold. The concentration ratio of the serine in Experiment I and alanine in Experiment II is close to one, indicating the reliability of the technique employed, since these amino acids were present in equal concentrations both in the normal incubating medium and in the modified medium. The amino acids present in medium B_1D were analysed by the amino acid analyzer, and none of them were found to have a concentration in excess of 0.5 mM, excepting glutamine which was 2.1 mM.

Out of the nine amino acids whose uptake into the cells are significant, only three amino acids have been selected for an elaborate study in this investigation. These are 1) the simplest and smallest amino acid, glycine, 2) the aromatic amino acid, phenylalanine, and 3) the basic amino acid, histidine.

TABLE 3

THE AMINO ACID UPTAKE STUDIED WITH AN AMINO ACID ANALYZER

		Cellular Amino Acid Concentrations		
		Cells Incubated in Normal medium (pmol/μg)	Cells Incubated in Modified medium (pmol/μg)**	Concentration Ratio
Exp I	*Aspartic acid	14.8	17.0	1.14
	Serine	4.7	4.5	0.95
	*Glutamic acid	110.8	115.3	1.04
	*Glycine	19.2	66.7	3.47
	*Alanine	9.8	68.2	6.96
	*Leucine	9.8	32.5	3.32
Exp II	*threonine	10.5	3.7	0.35
	*Serine	4.7	26.0	5.53
	*Glycine	19.2	52.8	2.75
	Alanine	9.8	10.0	1.02
	*Valine	undetectable amount	10.0	>2.5#
	*Methionine	undetectable amount	15.2	>3.3#
	*Phenylalanine	undetectable amount	19.7	>4.9#
Exp III	*Histidine	undetectable amount	46.4	>11.6#
	*Tryptophan	undetectable amount	50.4	>12.6#
	*Arginine	20.5	38.4	1.87
	*Lysine	undetectable amount	undetectable amount	---

**Certain specific amino acids (denoted by *) have been added in the normal medium, with each of them having a concentration of 10mM.

#Evaluation was made by assuming the detectable limit as 4.0 picomole/μg protein.

Amino Acid Uptake Studied by Labelled Amino Acids

Study I - Effects of Concentrations of Amino Acid in the Incubation Media on Amino Acid Uptake

The cellular concentration of each of the three amino acids studied, glycine, phenylalanine and histidine, was found to increase with the concentration of that amino acid in the incubation medium. All three amino acids studied reveal saturation characteristics in uptake (Figure 13). Histidine has the highest concentration maximum of 800 picomole per µg of protein, whereas the maximum cellular concentrations of glycine and phenylalanine are 350 pmol/µg and 260 pmol/µg respectively.

Study II - Effects of Concanavalin A (Con A) on Amino Acid Uptake

The effects of Con A on glycine uptake in normal and anaplastic cancer cells in tissue culture are shown in Figure 14. Con A inhibited the glycine uptake of cancer cells up to 43% at the concentration of 750 µg/ml. Con A showed an inhibitory effect on the glycine uptake of normal cells also. However, at concentrations of 500 and 750 µg/ml, the inhibitory effect of Con A on the glycine transport is higher in the cancer cells.

The results of similar experiments concerning phenylalanine uptake are presented in Figure 15. A maximum inhibition of 28% on phenylalanine uptake in cancer cells was expressed at the Con A concentration of 500 µg/ml. This maximum inhibition, however, is not significantly different in a statistical sense from the degree of inhibition produced in the normal cells.

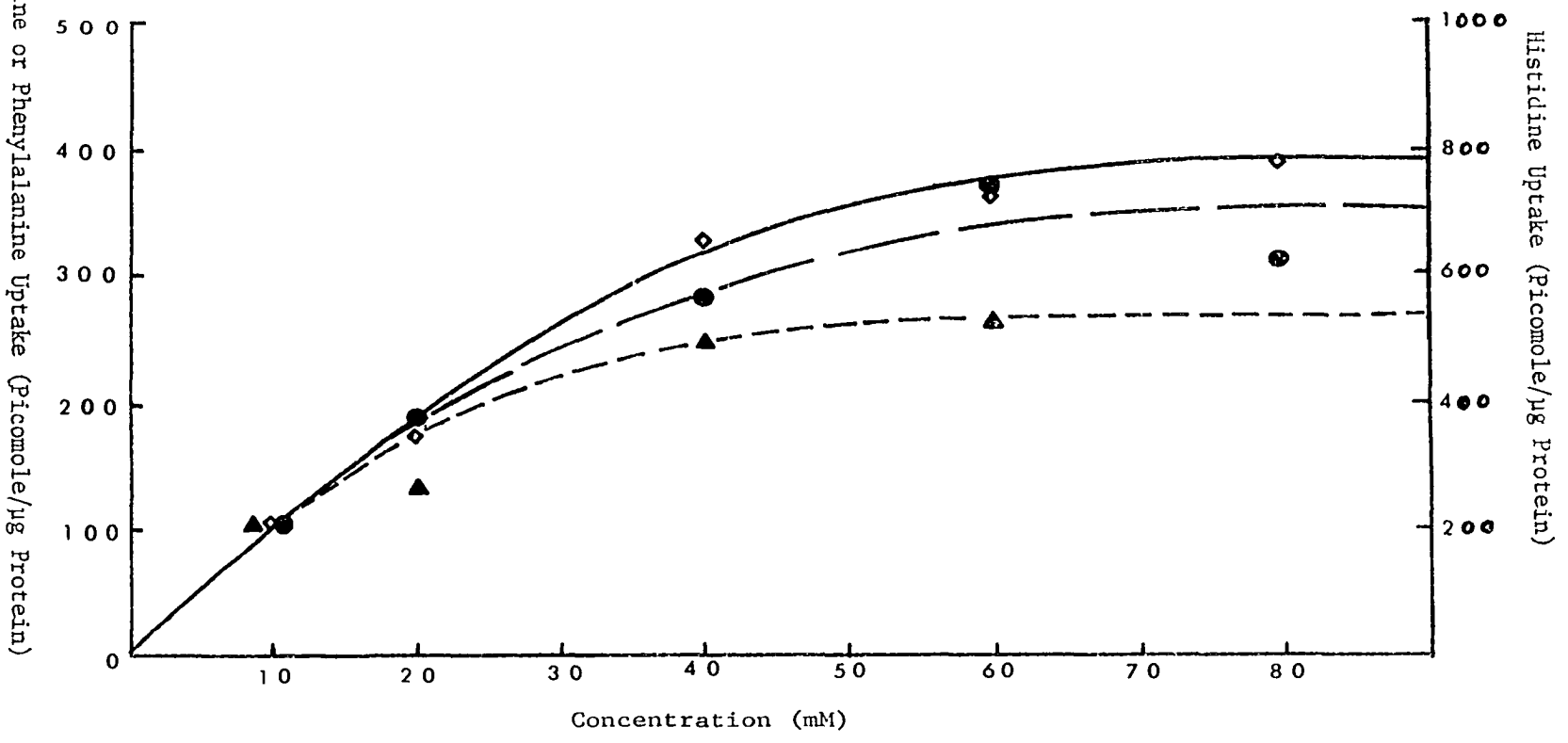

Figure 13. The saturation curves for glycine (●— —— —), phenylalanine (▲---) and histidine (◇————) uptake in anaplastic carcinoma cells.

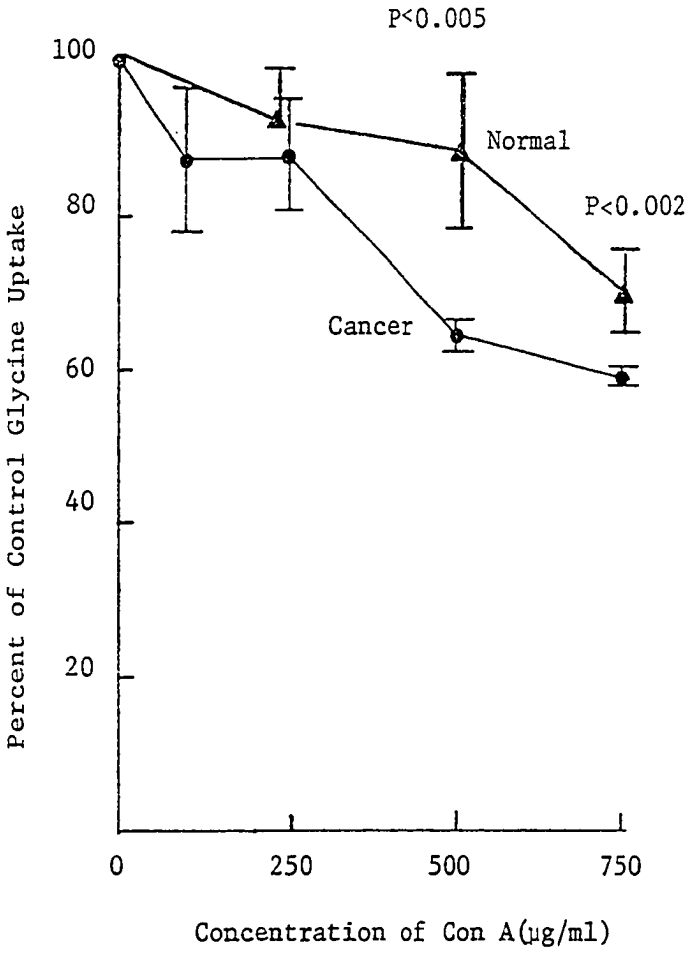

Figure 14. Effects of Con A on glycine uptake in normal fibroblasts and anaplastic carcinoma cells. The means, plus and minus standard errors, represent 4 experiments with cancer cells and 3 experiments with the normal cells. P values of student t test at two Con A concentrations are shown in the graph.

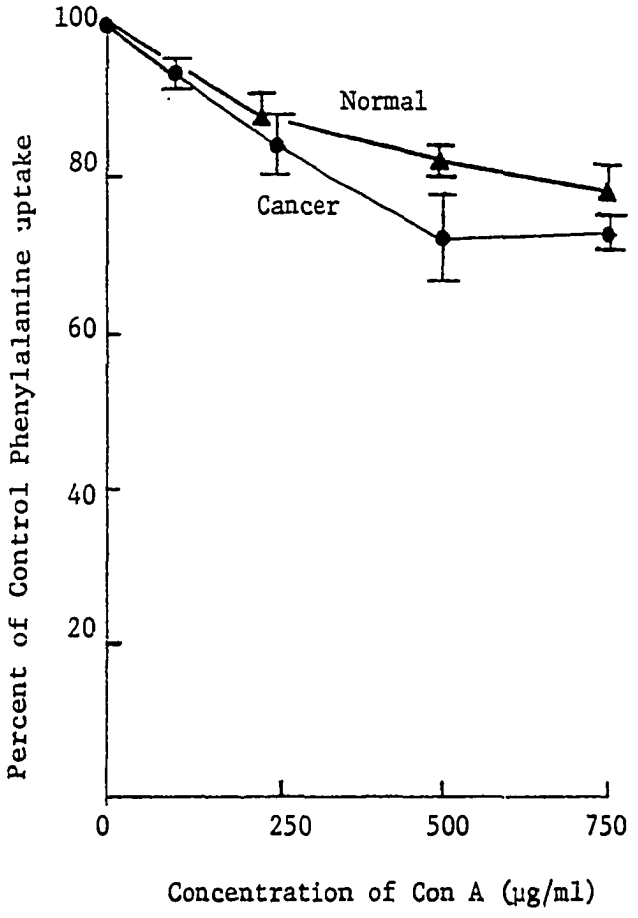

Figure 15. Effects of Con A on phenylalanine uptake in normal fibroblasts and anaplastic carcinoma cells. The means, plus and minus standard errors represent 4 experiments with cancer cells and 3 experiments with the normal cells.

The effect of Con A on histidine uptake in cancer cells is demonstrated in Figure 16. The maximum inhibition of histidine was 18% and that occurred at a Con A concentration of 250 µg/ml. The uptake of histidine in normal cells showed little effect by Con A treatment, the maximal inhibition being 6% of the control level. The difference in the inhibitory effects of Con A on normal and cancer cells is statistically significant.

Figures 17a and 17b are the phase contrast photographs of cancer cells. Photograph in Figure 17a, taken prior to the administration of Con A, serves as the control. After 1 hr incubation with Con A (750 µg/ml) and another hour of incubation in medium B_1D but free from Con A, the same cells were photographed again and this represents Figure 17b. It is to be noted that the morphology of the cells has been altered remarkably. The pseudopodium-like projections were withdrawn and most of the cells take up a spherical shape. Besides the change in the shape, there was no direct sign of cytotoxicity, such as vacuolation, swelling or disintegration of the cell. Furthermore, the slope of growth curves did not show any significant change after 1 hr of incubation with Con A solution (Figure 18). It seems, therefore, that Con A treatment in these experimental conditions imposed a shock to the cells temporarily and they recovered subsequently.

Study III - Effects of Polylysine on Amino Acid Uptake

Figure 19 shows the inhibition of glycine uptake by polylysine in normal and anaplastic carcinoma cells. Glycine uptake was reduced by polylysine treatment to about the same degree in both types of cells. About 30% inhibition was observed in cancer as well as in normal cells

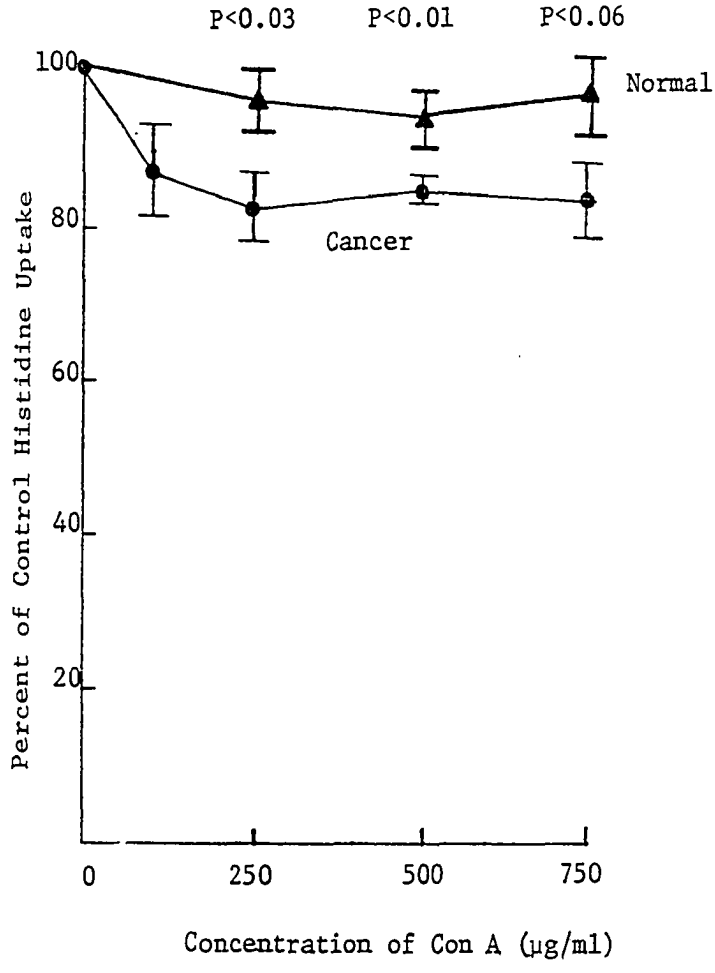

Figure 16. Effects of Con A on histidine uptake in normal fibroblasts and anaplastic carcinoma cells. The means, plus and minus standard errors represent 4 experiments with cancer cells and 3 experiments with the normal cells. P values of student t test at three Con A concentrations are shown in the graph.

Figure 17a. The anaplastic carcinoma cells in tissue culture observed under a phase contrast microscope prior to Con A incubation (320x). The finest division of the scale represents 5μ.

Figure 17b. The anaplastic carcinoma cells in tissue culture following 1 hr of incubation with 750 μg/ml Con A and 1 hr of incubation with medium B_1D. Same colony of cells as in Figure 17a was photographed under a phase contrast microscope (320x).

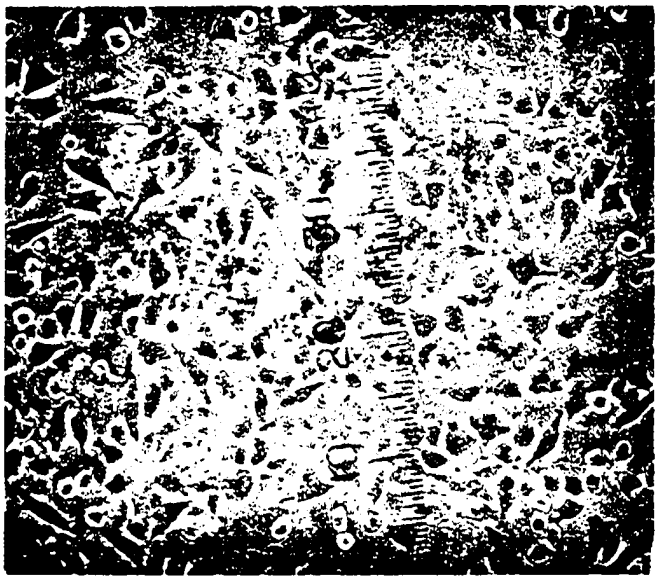

Fig 17a

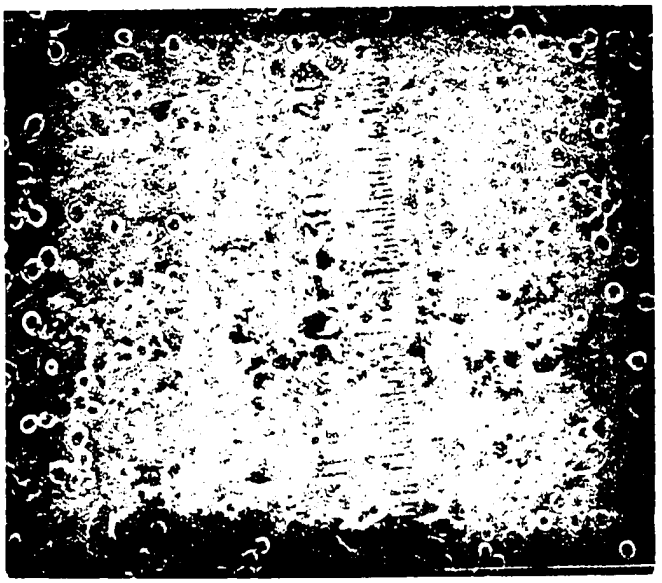

Fig 17b

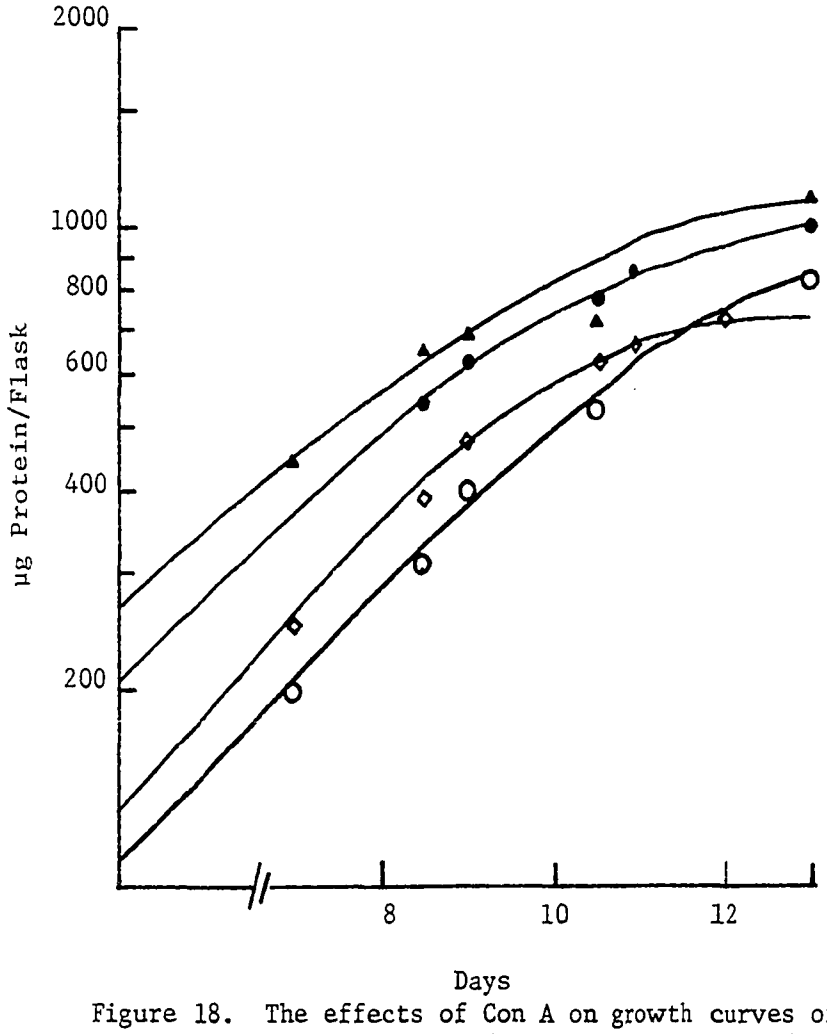

Figure 18. The effects of Con A on growth curves of anaplastic carcinoma cells in culture. ◇: 0µg/ml Con A; O: 500 µg/ml Con A; ▲: 750 µg/ml Con A; ●: 1,000 µg/ml Con A. The incubation with Con A lasted for 1 hr and followed by the normal growth medium.

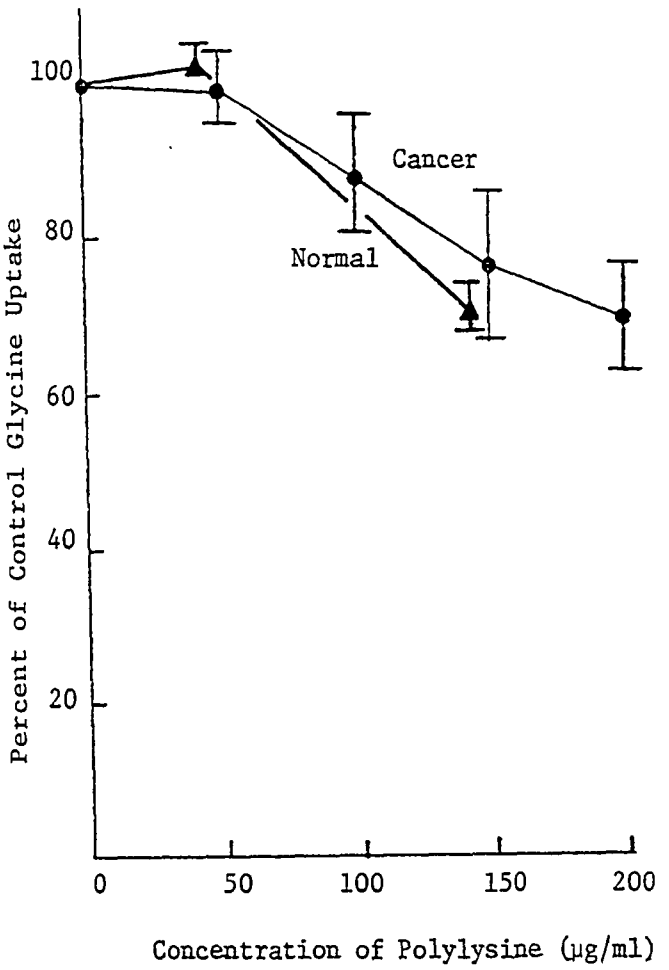

Figure 19. Effects of polylysine on glycine uptake in normal fibroblasts and anaplastic carcinoma cells. The means, plus and minus standard errors represent 4 experiments with cancer cells and 3 experiments with normal cells.

with a polylysine concentration of 150 µg/ml, whereas a 50 µg/ml concentration of polylysine did not show any inhibition.

The polylysine effect on phenylalanine uptake is demonstrated in Figure 20. Cancer cells preincubated with 150 µg/ml of polylysine showed a 30% inhibition on phenylalanine uptake, while in normal cells only a 10% inhibition was observed at this concentration of polylysine. Further increase of polylysine did not cause any further inhibition of phenylalanine transport in cancer cells.

Figure 21 displays the results of similar experiments on histidine uptake. Concentration of polylysine at 50 µg/ml reduced the histidine uptake in cancer cells only by 13% and a 150 µg/ml concentration of polylysine showed about a 20% inhibition, which was about the maximum inhibition that polylysine could impose on histidine uptake. Histidine uptake in normal cells was hardly affected by polylysine.

The possible morphological changes of cultured cells associated with polylysine treatment were studied by observation under the phase contrast microscope. The photograph in Figure 22a is the control picture taken right before polylysine treatment. After a 10 min incubation with 150 µg/ml polylysine and subsequent 1 hr incubation with regular medium, the photograph in Figure 22b was taken. The proportion of rounded cells (including those cells with very short projections) in population was shown to have increased. However, eight days later, the same flask of cells was photographed (Figure 23). This photograph reveals a densely growing, confluent layer with most cells attached, indicating that no permanent damage had been caused by polylysine.

Figure 24 is a high magnification photomicrograph of cells after

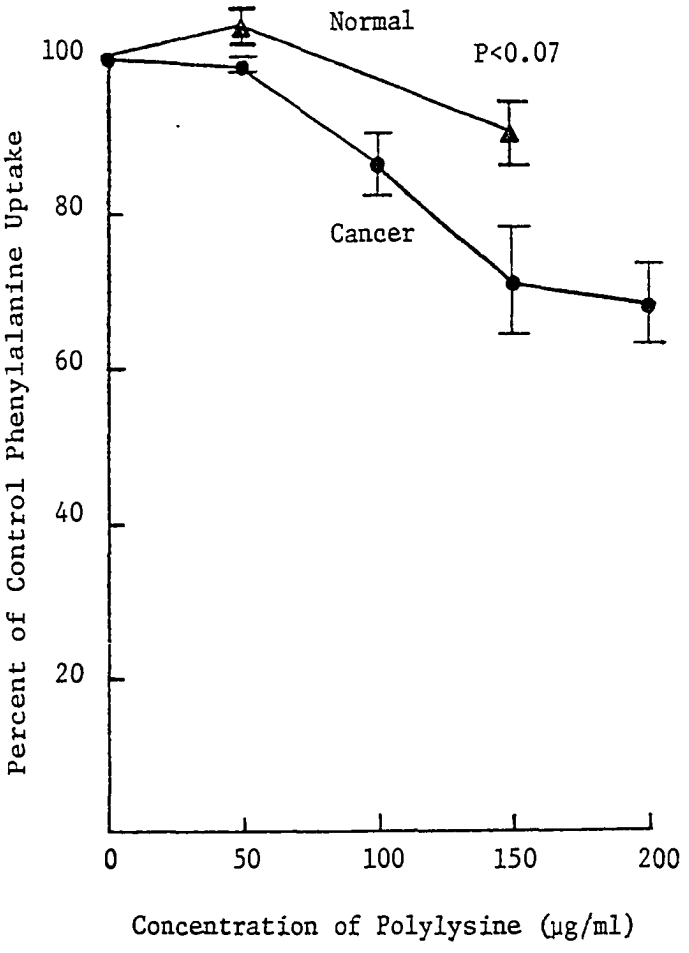

Figure 20. Effects of polylysine on phenylalanine uptake in normal fibroblasts and anaplastic carcinoma cells. The means, plus and minus standard errors represent 4 experiments with cancer cells and 3 experiments with normal cells. A P value of student t test is shown in the graph.

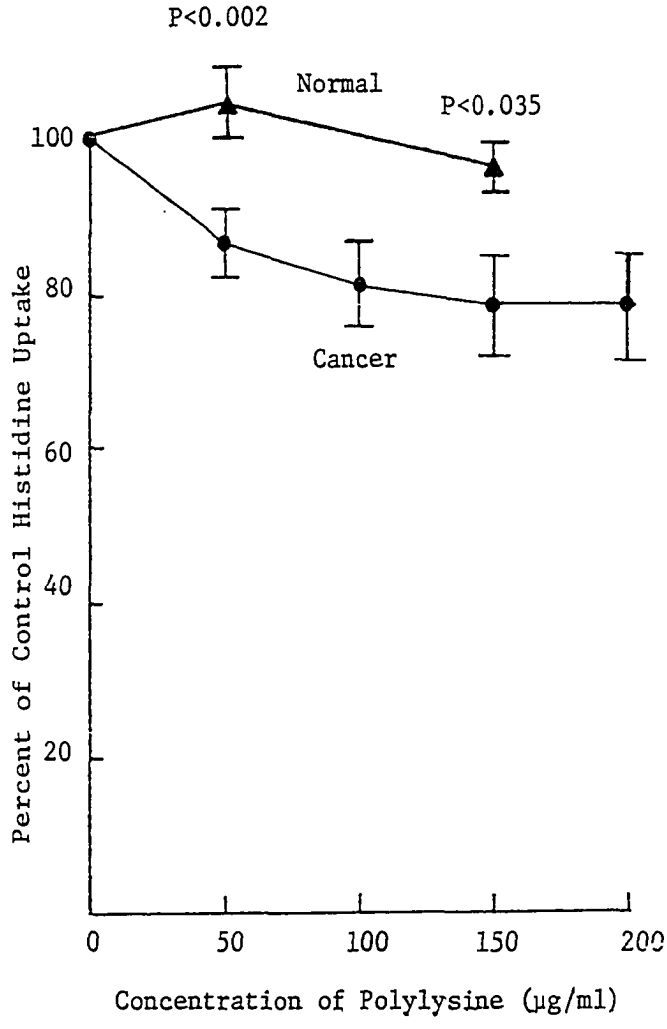

Figure 21. Effects of polylysine on histidine uptake in normal fibroblasts and anaplastic carcinoma cells. The means, plus and minus standard errors are from 4 experiments with cancer cells and 3 experiments with normal cells. P values of student t test at two polylysine concentrations are shown in the graph.

Figure 22a. The anaplastic carcinoma cells in tissue culture observed under a phase contrast microscope prior to polylysine incubation (320x). The finest division of the scale represents 5μ.

Figure 22b. The anaplastic carcinoma cells in tissue culture following 10 min incubation with 150 μg/ml polylysine and 1 hr incubation with medium B_1D. Same colony or cells as in Figure 22a was photographed under a phase contrast microscope (320x).

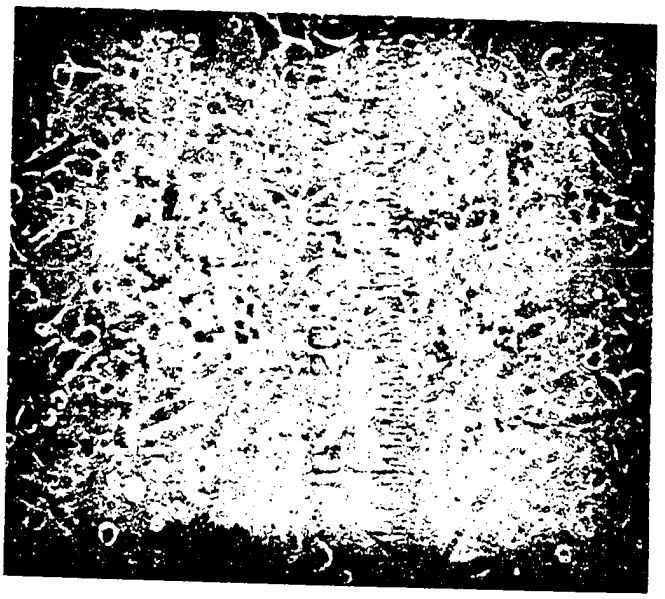

Fig 22 a

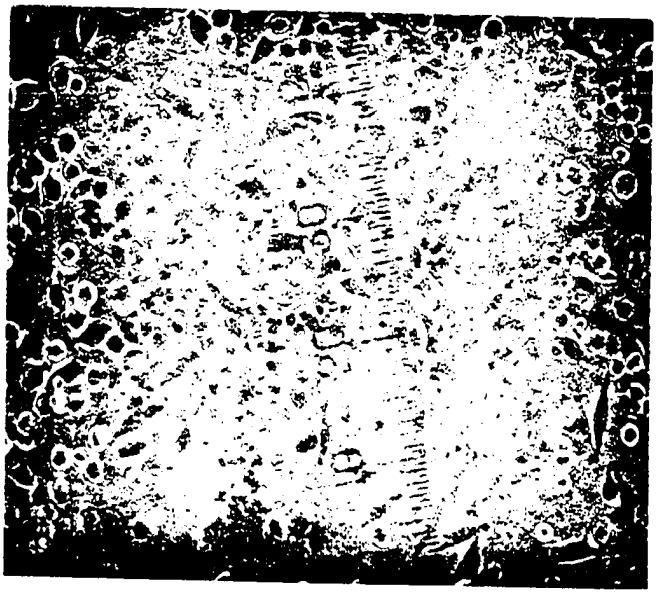

Fig 22 b

Figure 23. The follow-up picture of Figure 22b. The picture was taken 8 days after polylysine treatment. Same magnification as in Figure 22b.

Figure 24. High-magnification photomicrograph of anaplastic carcinoma cells in tissue culture after a 10 min incubation with 300 µg/ml polylysine and 1 hr incubation with medium B_1D (640x). The finest division of the scale represents 2.5µ.

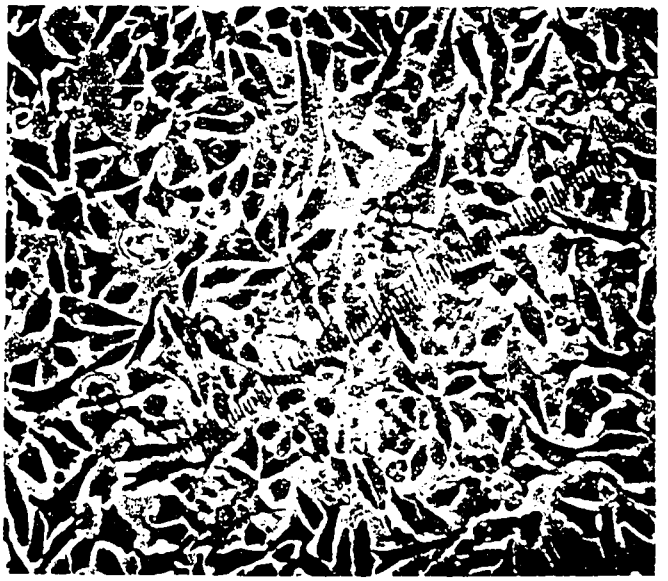

Fig 23

Fig 24

an incubation with polylysine (300µg/ml) for 10 min, followed by an incubation with the regular medium B_1D for 1 hr. Although some cells were round, no deterioration of cellular structures can be observed. Nevertheless, it was found that if cells were exposed to the same concentration of polylysine for 1 hr instead of 10 min, they develop coarse granules, vesicles and blebs in the cytoplasm, followed by their expansion and disintegration.

Study IV - Effects of Dinitrophenol (DNP) and Iodoacetate on Amino Acid Uptake

The results on the effects of the above metabolic inhibitors are presented in Table 4. All three amino acids studied were inhibited by these metabolic inhibitors. Iodoacetate showed a much larger inhibitory effect than DNP on the amino acid transport. The combination of iodoacetate and DNP had larger inhibitory effects on the uptake of all three amino acids tested. It was observed that a large percentage of cells detached from the culture flask and were lost during the washing process after incubation with the mixture of metabolic inhibitors, indicating that a larger percentage of the cells were killed. The results presented in Table 4 correspond to the smaller number of cells still attached to the substratum.

Study V - Effects of Temperature on Amino Acid Uptake

The uptake of glycine, phenylalanine and histidine in cancer cells was studied at 27°, 32° and 35°C. As shown in Figure 25, temperature had a very large effect on glycine uptake, the uptake increasing 55 picomole per µg protein per 10°C increment of temperature. The corresponding increases in the uptake of phenylalanine and histidine were

TABLE 4

THE EFFECTS OF DNP AND IODOACETATE ON GLYCINE, PHENYLALANINE AND HISTIDINE UPTAKE IN ANAPLASTIC CARCINOMA CELLS

	Glycine		Phenylalanine		Histidine	
	Concentration (pmol/µg protein)	% of Control Uptake	Concentration (pmol/µg protein)	% of Control Uptake	Concentration (pmol/µg protein)	% of Control Uptake
Control	270	100	191	100	212	100
DNP (0.1mM)	192	71	157	82	162	76
Iodoacetate (1.0mM)	133	58	143	75	118	56
DNP (0.1mM) and Iodoacetate (1.0mM)	119	44	118	62	113	51

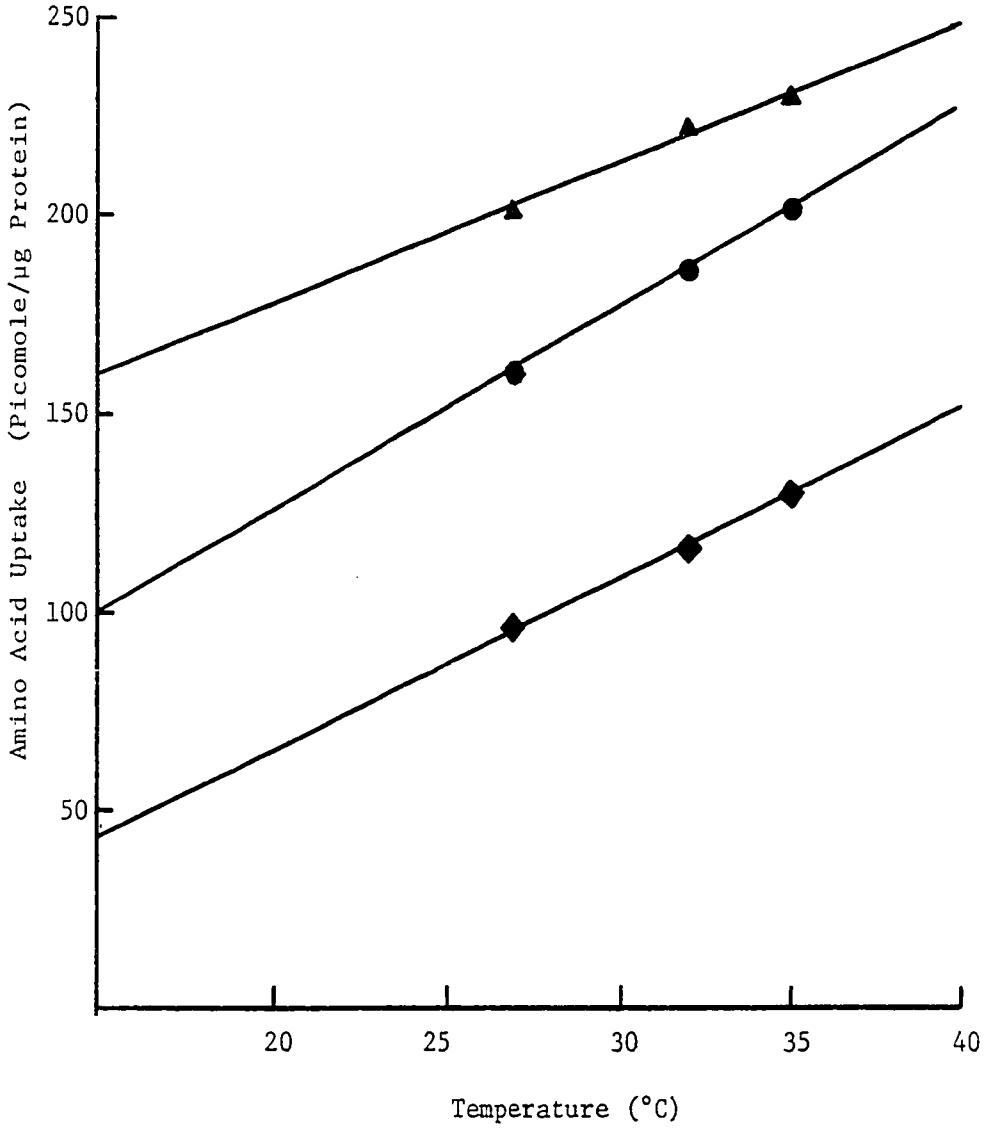

Figure 25. The effects of temperature on amino acid uptake in anaplastic carcinoma cells. ● stands for glycine uptake, ◆ for phenylalanine uptake and ▲ for histidine uptake.

45 pmol/μg and 35 pmol/μg respectively.

Figure 26 is a replot of the data in Figure 25 wherein the uptake values at 32°C and 35°C are expressed in proportion to the value at 27°C. The extrapolation of the graphs indicate that because of a 10°C increase in temperature the uptake of the three amino acids, glycine, phenylalanine and histidine, are increased by 31, 42 and 18% respectively. If the Q_{10} of uptake is defined as the ratio of uptake of amino acid at certain temperature and the uptake at temperature ten degrees lower, the Q_{10}'s of glycine, phenylalanine and histidine are 1.31, 1.42 and 1.18 respectively. The Q_{10}'s are considerably larger than unity.

Study VI - Effects of α-Methyl-D-Glucopyranoside (αMG) on Concanavalin A Inhibition of Amino Acid Uptake

The presence of 0.1M αMG counteracts the inhibitory action of Con A on amino acid uptake. As shown in Table 5 and 6, the addition of αMG into the preincubation medium invariably reduced the degree of inhibition caused by Con A in both the normal and malignant cells. The protective effect of αMG from the inhibition of Con A was excellent with regard to the transport of glycine and phenylalanine in normal cells, and glycine in cancer cells.

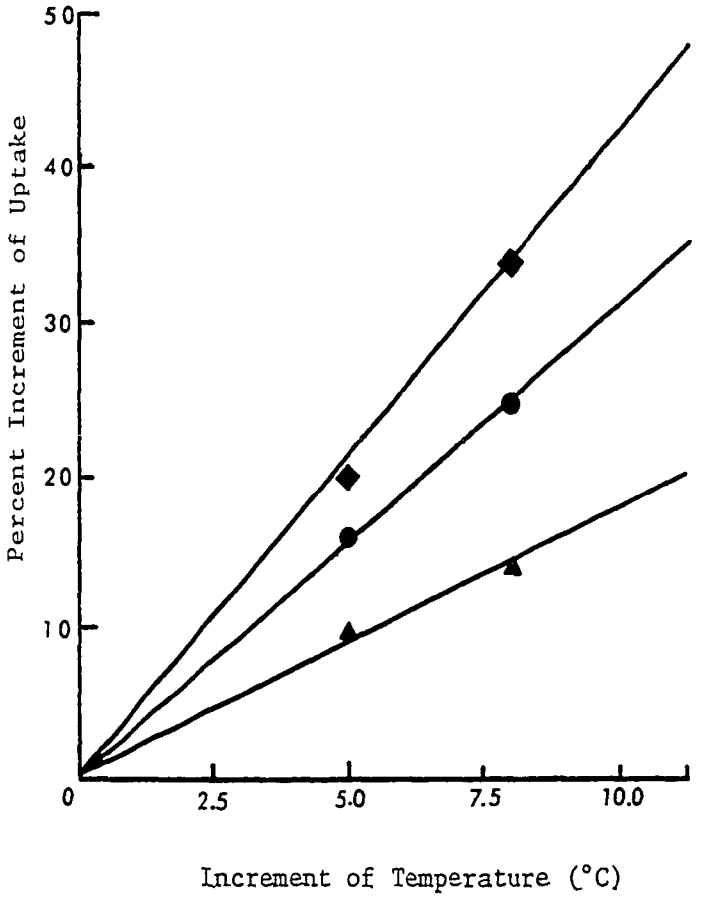

Figure 26. A replot of Figure 25. Ordinate: Percent increment of uptake with respect to the amino acid uptake at 27°C. Abscissa: Increment in temperature beyond 27°C. Symbols are the same as indicated in Figure 25.

TABLE 5

THE EFFECTS OF α-MG ON CON A INHIBITION OF GLYCINE UPTAKE

(Means and standard errors are given in the table)

	Cancer Cells		Normal Cells	
	Concentration (pmol/μg protein)	% of Control Uptake	Concentration (pmol/ μg protein)	% of Control Uptake
Control	210 ± 6	100	479 ± 16	100
Con A 150 g/ml	136 ± 12	65 ± 6	335 ± 25	70 ± 5
Con A 150 g/ml + MG 0.1M	198 ± 3	94 ± 1	469 ± 31	98 ± 6

TABLE 6

THE EFFECTS OF α-MG ON CON A INHIBITION OF PHENYLALANINE UPTAKE

(Means and standard errors are given in the table)

	Cancer Cells		Normal Cells	
	Concentration (pmol/μg protein)	% of Control Uptake	Concentration (pmol/μg protein)	% of Control Uptake
Control	233 ± 8	100	417 ± 3	100
Con A 150 μg/ml	163 ± 4	70 ± 2	327 ± 15	78 ± 3
Con A 150 μg/ml + MG 0.1M	194 ± 12	83 ± 5	442 ± 11	106 ± 3

CHAPTER IV

DISCUSSION

Discussion of Electrical Measurements

The significance of the present electrical measurements are two-fold. Firstly, the microelectrodes used in this study were extremely fine, e.g., the tip diameter was about 500 Å. The fineness of the tip enables the insertion of the microelectrode into the cell to be made with a minimum of dimpling of the cell membrane and/or damage to the cell. This is reflected by the fact that in many cases, the magnitudes of intracellular potential and membrane resistance monitored from successive punctures of the same cell were exactly the same. In addition, unlike the studies performed by others, the potentials measured in our systems were more stable and they remained stable for as long as several minutes. Such findings indicate that very little damage, if any, has been caused by the insertion of the microelectrode.

Secondly, the properties of the microelectrodes used in this study were characterized with respect to the change of tip potential caused by transferring the microelectrode from K-Ringer's solution to isosmotic Na-Ringer's solution. The Na-Ringer's solution simulates the extracellular fluid and the K-Ringer's solution the intracellular fluid. Therefore, the potential difference attributed by any change of the tip potential during insertion of the microelectrode into the cell can be evaluated. In this

study, all the intracellular potentials obtained from cellular punctures were corrected by subtracting from them the potential difference attributed by the tip potential change. This correction is necessary and yet rarely mentioned or simply neglected by previous investigators. Especially when the intracellular potential is of small magnitude, correction for the change in the tip potential itself can become even more important.

Electrical measurements of normal and malignant cells were carried out in two different systems. The in situ measurements of skin tissue showed that cancer cells had lower negative intracellular potential and higher membrane resistance than their normal counterparts. This low intracellular potential can hardly arise from any artefact of local membrane damage, because if that had been the case, the resistance should also have been lower, which is not the case. The same type of findings has been reported recently by other investigators (22, 24, 104) in different tissue preparations.

In the tumor cells, both the intracellular potential and the membrane resistance show much wider spreads in their magnitudes as compared to those in the normal epidermal cells. This is proposed to be due to the cells being at various stages of oncogenesis. This viewpoint is supported by the histological finding (Figure 2a) that in the solid tumor mass the neoplastic cells show varying degrees of differentiation.

With regard to the in vitro study, however, the carcinoma cells and normal fibroblasts did not have any large differences in their intracellular potential and membrane resistance values. The intracellular potentials of both the anaplastic carcinoma cells and the normal fibroblasts were very low, the mean of the former being -4.9 ± 0.4 mV and that of the

latter being -0.6 ± 0.5 mV. Extreme difficulty was encountered in measuring the intracellular potential and membrane resistance of very thin normal fibroblasts. Although statistically the measured mean potential of cancer cells was significantly different from the mean of normal cells, the possibility of an artefact cannot be ruled out. In a normal situation, the electrical current passes across the cell membrane through the electrolytes solution within the microelectrode. However, when the cell is damaged during insertion, the current can go through the membrane which is sealing around the microelectrode and results in a smaller magnitude of voltage drop monitored by the inserted microelectrode. This shunting effect by microelectrode insertion may be at least partly responsible for the low potential monitored from normal fibroblasts. This can be understood when one considers the difficulty involved in placing a microelectrode right in between the two very closely opposed cytoplasmic membrane. It seems quite likely that a slight degree of damage on the membrane might have been created in the electrical measurements of normal cells. Therefore, no unambiguous conclusion can be reached for comparing the potential measurements of anaplastic carcinoma cells with those of the corresponding fibroblasts. There may not be any difference between the in vitro intracellular potentials of the normal and cancer cells studied here. Indeed, not all the cancer cells studied so far have lower intracellular potential than their normal counterparts. Shanne (105) has shown that the intracellular potentials of human cervical cancer, human skin cancer and rat fibrosarcoma did not differ from their normal analogues.

In parallel with our results on membrane resistance of anaplastic carcinoma cells and fibroblasts, Borek et al (24) have found that the

membrane resistance of fibroblasts and their corresponding malignant cells did not vary with each other when measured in the in vitro system. They observed that the magnitudes of the membrane resistances in the hamster fibroblast, rat fibroblast, mouse 3T3 cell and their counterparts were almost identical.

Since the membrane resistance is a measure of ionic permeation, the high resistance of skin tumor cells indicates a decrease in the rate of ionic movements across the membrane, perhaps as a result of some structure alteration in the membrane. Loewenstein (21) proposed that normal cells grow and differentiate in an organized way under some kind of control signals. The channel of signal, however, is sealed off in the membrane of malignant cells. In view of such a hypothesis, an increased membrane resistance of cancer cells may be considered to cause not only a blockage of the so-called control signal but also to restrict the movements of ions. However, the control signal is still a purely hypothetical term without any substantial identity. Nevertheless, similarity in the magnitudes of membrane resistance of anaplastic carcinoma cells and normal fibroblasts may be considered to indicate that there is no major difference in the net ionic movements among these two groups of cells.

Thus, the measurements of intracellular potential and membrane resistance can be effectively used in differentiating skin tumor cells from normal cells, since marked electrical differences do exist between these two groups of cells. On the other hand, the intracellular potential and membrane resistance in anaplastic carcinoma cells are not significantly different from those of normal fibroblasts. However, the existance of about the same resistance between certain tumor and normal cells does

not exclude the possibility of membrane alteration. The lack of difference in these two electrical parameters of the anaplastic carcinoma cells from those of the normal fibroblasts may mean that the levels of the transport of ions are not different in these two groups of cells. But, perhaps in some other transport characteristics, the in vitro anaplastic carcinoma cells are distinguishable from their normal counterparts. This leads to the second part of the present investigation, i.e., the study of amino acid transport in these groups of cells. The reason for the lack of a general pattern of alteration in electrical potential and resistance in malignant transformation is probably related to the individuality of cancers.

Discussion on the Study of Amino Acid Uptake

It was found that Con A at concentrations of 500 μg/ml or higher inhibited the uptake of glycine, phenylalanine and histidine in transplantable anaplastic carcinoma cells. In the normal fibroblasts, however, the inhibition of glycine and histidine uptake is much less than that in carcinoma cells. In other words, Con A produced a selective inhibition of glycine and histidine uptake in the cancer cells.

Con A has been shown to bind specifically with α-D-mannopyranosyl, α-D-glucopyranosyl, and β-D-fructofuranosyl residues in polysaccharide as well as in mono- and oligosaccharides (43, 58, 106). Since the cell surface is covered with glycoprotein or glycolipid, Con A then can conceivably bind with the carbohydrate residues of the surface membrane. Besides, immunofluorescence study (107) demonstrated the binding of Con A on the surfaces of various cells by the appearance of a zone of fluorescence surrounding the cells. Furthermore, electron microscopic study using

ferritin-conjugated Con A (108) also revealed the binding of Con A on the cell surfaces of both normal and cancer cells. We have observed that αMG, a carbohydrate similar to α-D-glycopyranose structurally, counteracted the inhibitory effect of Con A on the uptake of amino acids in both normal as well as carcinoma cells. This finding suggests that the inhibitory effect of Con A on amino acid uptake results from the binding of an αMG-like binding site of Con A to the membrane surface, since the occupance of the αMG binding site eliminated the Con A action completely. This is in agreement with the general belief that the action of Con A is caused by binding to the carbohydrate moiety of the cell membrane. αMG, in addition, has been demonstrated to reverse the agglutination of cancer cells caused by Con A, thus our result seems to indicate a close link between the inhibition of amino acid transport and agglutinability. Unfortunately, this relationship cannot be tested without ambiguity because the cells are grown in a monolayer, and they are attached to the substratum.

Identical results were obtained on the effects of polylysine on amino acid uptake. Uptake of all three amino acids studied were inhibited considerably by polylysine in the anaplastic carcinoma cells. Selective inhibitions were found only in uptake of phenylalanine and histidine. Uptake of glycine in normal cells had even a slightly higher degree of inhibition than in cancer cells. Since polylysine is bound to the membrane (72), and does not penetrate into the cell within a short period of time (74), an analogous explanation for the action of Con A seems pertinent.

From the results of Con A and polylysine studies, we are tempted

to make the following hypothesis: the difference in the structure of the surface membrane between normal and transformed cells can be reflected by differential inhibitions of Con A and polylysine on amino acid uptake. It is proposed that the location of the amino acid transport sites in relation to the binding sites for Con A and polylysine has become altered by the malignant transformation, and the uptake of a particular amino acid is inhibited if its transport site is blocked by binding of Con A or polylysine. As shown in Figure 27, in anaplastic carcinoma cell, Con A and polylysine binding sites coincide or are adjacent to glycine, histidine and phenylalanine transport sites. Yet, in normal cells Con A and polylysine binding sites are superimposed with phenylalanine and glycine transport sites respectively. The histidine transport site in normal cell is neither adjacent to the polylysine binding site nor to the Con A binding site, and consequently histidine uptake in normal cells is not inhibited by the treatment with either Con A or polylysine. Since the glycine transport site is closely associated with the polylysine binding site on the surface membrane of the normal cell, as illustrated in Figure 27, the binding of polylysine on the normal cell causes an inhibition of glycine uptake of normal cells, but no effect on either the phenylalanine or histidine uptake.

This hypothesis does not require a net increase of binding sites for Con A or polylysine but a change in their relative locations. It is in good agreement with the findings that the number of Con A binding site of membrane surfaces of normal as well as transformed cells were the same (70, 71, 108).

The direct evidence that rearrangement of membrane binding sites

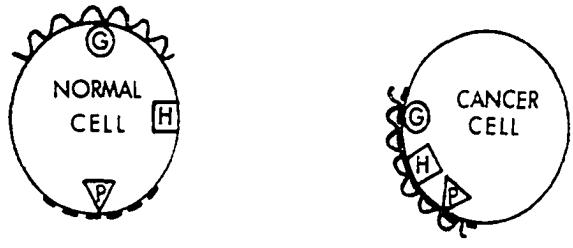

Figure 27. A model illustrating the difference between the cell surface of a normal mouse fibroblast and an anaplastic carcinoma cell, particularly with respect to the relative location of the amino acid transport sites to the Con A and polylysine binding sites on the membrane surfaces. G denotes the glycine-, P the phenylalanine- and H the histidine transport sites. The dashed line represents the Con A molecule and the spiral configuration the polylysine molecule. The Con A and polylysine binding sites are located on the surface to which the Con A and polylysine molecules are bound.

take place in transformed cells was provided by Nicholson's electron microscopic observation using ferritin conjugated Con A (Fer-Con A) (108). The distribution of Fer-Con A on cell surfaces of normal mouse 3T3 cells revealed an essentially random distribution of single Fer-Con A molecules, whereas the SV40 virus-transformed 3T3 cells showed that the Fer-Con A almost exclusively present in large, randomly dispersed clusters. The clustering indicates redistribution of membrane Con A binding sites.

The presence of transport sites on the cell surface is based on the assumption that a carrier mediated transport system is associated with the uptake of amino acids. Our experimental results have indicated that in the cells which we have studied, the uptake of amino acids, glycine, phenylalanine and histidine are mediated through an active transport process. Our evidence is derived from the following observations: 1) Metabolic inhibitors, e.g., DNP and iodoacetate, caused significant inhibition of amino acid uptake, indicating that the transport process is metabolically linked. 2) The study of the temperature effects on amino acid uptake in cancer cells has shown a Q_{10} of 1.31, 1.42 and 1.18 for glycine, phenylalanine and histidine respectively. The Q_{10} values are all higher than that expected from simple passive diffusion.* 3) The saturation curves of glycine, phenylalanine and histidine uptake in cancer cells are the manifestations of some carrier mediated transport processes. 4) The estimated values of intracellular amino acid concentrations are suggestive of an uphill transport of amino acids in cancer cells. The observed values of glycine, phenylalanine and histidine concentrations are 281, 153 and 205 picomole/μg protein respectively.

---

* See appendix.

The estimated average cell volume of the anaplastic carcinoma cell is 2.6×10^{-9} ml. Protein analysis of known numbers of cells indicates that 1 µg of cellular protein corresponds to 4.6×10^{-6} ml of cell volume. Based on this relationship the intracellular concentrations of glycine, phenylalanine and histidine are calculated to be 105, 33 and 45 mM respectively, which are well above the concentration of the amino acid in the incubating medium. Thus, the accumulation of at least these three amino acids in the cells, at concentrations higher than that in the incubation medium, is most likely to be via an active transport process.

Before drawing the conclusions, I would like to restate the questions asked at the start of this investigation. They are:

1) Are the intracellular potential and membrane resistance in the tumor cells different from those in the normal cells?

2) Do the surface interacting agents such as Con A and polylysine exert different degrees of effect on the uptake of amino acid in tumor cells and normal cells?

The following answers to the above questions comprise the conclusion of this study:

1) The intracellular potential and membrane resistance of the chemically induced skin tumor cells are markedly different from those of the normal cells. The cancer cells have a lower negative intracellular potential and higher membrane resistance than their normal counterparts. The intracellular potential and membrane resistance of the anaplastic carcinoma cells, however, aren ot significantly different from those of normal fibroblasts.

2) Con A has greater inhibitory effects on the uptake of glycine and histidine in anaplastic carcinoma cells than in normal fibroblasts. Polylysine, on the other hand, exerts a larger inhibition on the uptake of phenylalanine and histidine in cancer cells than in normal cells.

The high temperature coefficients of the uptake of amino acids are suggestive of some active process being involved in the cellular transport of the three amino acids studied. As a difference in the membranes of cancer and normal cells, it is proposed that some rearrangement in the transport sites may be taking place during transformation.

CHAPTER V

SUMMARY

This thesis described two types of experiments. The first were experiments with electrical measurements and the second were concerned with amino acid transport.

1. With the aid of ultrafine tipped glass microelectrodes tip diameter about 500 Å, intracellular electrical measurements were carried out in two different groups of normal and malignant cells. a) In situ skin tumor cells have lower magnitudes of negative intracellular potential and yet higher magnitude membrane resistance than do normal epidermal cells. Furthermore, the intracellular potential of the tumor cells varies widely between -5 and -32 mV, whereas the range of potential of the normal cells is limited to the narrow range of -25 and -34 mV. The means of the intracellular potentials of tumor cells and normal cells are -18.5 ± 1.0 mV and -31.5 ± 0.3 mV respectively. The difference between these two means is statistically highly significant ($P<10^{-12}$). The resistance of the tumor cells also shows a wider spread in its magnitude than that in the normal cells. The mean membrane resistance is 6.5 ± 0.6 MΩ in tumor cells, and 3.0 ± 0.1 MΩ in normal cells. The difference of resistance in normal and malignant epidermal cells is statistically highly significant ($P<10^{-8}$). The wider spreads in the magnitudes of intracellular potential and membrane

resistance of tumor cells are proposed to be due to the cells being at various stages of oncogenesis. b) The in vitro study of anaplastic carcinoma cells and normal fibroblasts does not show any large differences in their intracellular potential and membrane resistance values. The intracellular potentials of both the anaplastic carcinoma cells and the normal fibroblasts are very low. The mean intracellular potential of the cancer cells is -4.9 ± 0.4 mV and that of the normal cells is -0.6 ± 0.5 mV. The mean membrane resistance is 3.4 ± 0.4 MΩ in anaplastic carcinoma cells, and 2.3 ± 0.4 MΩ in normal fibroblasts. The difference of resistance in normal and malignant cells is statistically insignificant.

2. Concanavalin A (Con A) has greater inhibitory effects on the uptake of glycine and histidine in anaplastic carcinoma cells than in normal fibroblasts. At a concentration of 500 μg/ml, Con A inhibits 36% of glycine uptake in cancer cells but only 12% in normal cells. With the same concentration of Con A, histidine uptake is inhibited by 15%, whereas only 6% inhibition is exhibited in normal cells. The inhibitory effect of Con A is antagonized by α-methyl-D-glucopyranoside (α-MG).

3. The inhibition on the uptake of phenylalanine and histidine by polylysine is much larger in the anaplastic carcinoma cells than in the normal cells. At a concentration of 150 μg/ml, polylysine shows a 30% inhibition of phenylalanine uptake in the cancer cells, while the inhibition of the uptake of the same amino acid in the normal cells is only 10%. The uptake of histidine in cancer cells is inhibited by 20%, whereas that in the normal cells is hardly affected by polylysine.

4. The uptake of amino acids in tumor cells is greatly reduced by metabolic inhibitors. Increases in the temperature of the bathing

medium produce significantly large increases in the uptake of the amino acids. These results suggest that some active process is involved in the transport of the three amino acids into the cells.

5. A model is postulated to interpret the differential effects exerted by Con A and polylysine on the transport of some amino acids.

BIBLIOGRAPHY

1. Wallach, D. F. H. 1968 Cellular Membranes and Tumor Behavior: A New Hypothesis. Microbiology 61:866.

2. Coman, D. R. 1944 Decreased Mutual Adhesiveness, A Property of Cells from Squamous Cell Carcinomas. Cancer Res. 4:625.

3. Abercrombie, M. and Ambrose, E. J. 1962 The Surface Properties of Cancer Cells: A Review. Cancer Res. 22:525.

4. Abercrombie, M. and Ambrose, E. J. 1958 Interference Microscope Studies of Cell Contacts in Tissue Culture. Exp. Cell Res. 15:332.

5. Abercrombie, M. and Heaysman, J. E. M. 1954 Social Behavior of Cells in Tissue Culture. II. Monolayering of Fibroblasts. Exp. Cell Res. 6:293.

6. Abercrombie, M., Heaysman, J. E. M. and Karthauser, H. M. 1957. Social Behavior of Cells in Tissue Culture. III. Mutual Influence of Sarcoma Cells and Fibroblasts. Exp. Cell Res. 13 276.

7. Temin, H. M. and Rubin, H. 1958 Characteristics of an Assay for Rous Sarcoma Virus and Rous Sarcoma Cells in Tissue Culture. Virology 6:669.

8. Sanford, K. K. 1968 in Cancer Cells in Culture. ed. Katsuta, H. pp. 281-289. (Univ. of Tokyo Press and University Park Press)

9. Curtis, A. S. G. 1961 Control of Some Cell-contact Reactions in Tissue Culture. J. Nat. Cancer Inst. 26:253.

10. Ambrose, E. J., James, A. M. and Lowick, J. H. B. 1956 Differences Between the Electrical Charge Carried by Normal and Homologous Tumor Cells. Nature 177:576.

11. Lowick, J. H. B., Purdom, L., James, A. M. and Ambrose, E. J. 1961 Some Microelectrophoretic Studies of Normal and Tumor Cells. J. Roy. Microscop. Soc. 80:47.

12. Purdom, L., Ambrose, E. J. and Klein, G. 1958 A Correlation Between Electrical Surface Charge and Some Biological Characteristics During the Stepwise Progression on a Mouse Sarcoma. Nature 181:1586.

13. Ben-Or, S., Eisenberg, S. and Doljanski, F. 1960 Electrophoretic Mobilities of Normal and Regenerating Liver Cells. Nature 188:1200.

14. Doljanski, F. 1968 The Electrophoretic Mobility of Normal and Malignant Cells. Harefuah 75:443.

15. Ohta, N., Pardee, A. B., MuAuslan, B. R. and Burger, M. M. 1968 Sialic Acid Contents and Controls of Normal and Malignant Cells. Biochim Biophys. Acta 158:98.

16. Weiss, L. 1967 in The Cell Periphery, Metastasis and Other Contact Phenomena, ed. Neuberger, A. and Tatum, E. L. pp. 268-270 and 303 (North-Holland Publishing Co.)

17. Borle, A. B. and Loveday, J. 1968 Effects of Temperature, Potassium and Calcium on the Electrical Potential Difference in HeLa Cells. Cancer Res. 28:2401.

18. Johnstone, B. M. 1959 Micro-Electrode Penetration of Ascites Tumor Cells. Nature 183:411.

19. Aull, F. 1967 Measurement of Electrical Potential Difference Across the Membrane of the Ehrlich Mouse Ascites Tumor Cell. J. Cell. Physiol. 69:21.

20. Fritz, M. E. and Nahmias, A. J. 1972 Reversed Polarity in Transmembrane Potentials of Cells Infected with Herpes Viruses (36320) Proc. Soc. Exp. Biol. Med. 136:1159.

21. Loewenstein, W. R. and Kanno, Y. 1967 Intercellular Communication and Tissue Growth. I. Cancerous Growth. J. Cell Biol. 33: 225.

22. Jamakosmanovic, A. and Loewenstein, W. R. 1968 Cellular Uncoupling in Cancerous Thyroid Epithelium. Nature 218:775.

23. Jamakosmanovic, A. and Loewenstein, W. R. 1968 Intercellular Communication and Tissue Growth. III. Thyroid Cancer. J. Cell Biol. 38:556.

24. Borek, C., Higashino, S. and Loewenstein, W. R. 1969 Intercellular Communication and Tissue Growth IV. Conductance of Membrane Junctions of Normal and Cancerous Cells in Culture. J. Membrane Biol. 1:274.

25. Sheridan, J. D. 1970 Low-Resistance Junctions Between Cancer Cells in Various Solid Tumor. J. Cell Biol. 45:91.

26. Van Slyke, D. D. and Meyer, G. M. 1913 The Fate of Protein Digestion Products in the Body. III. The Absorption of Amino-acids from the Blood by the Tissues. J. Biol. Chem. 16:197.

27. Christensen, H. N. and Streicher, J. A. 1949 Concentrations of Amino Acids by the Excised Diaphragm Suspended in Artificial Media. I. Maintenance and Inhibition of the Concentrating Activity. Arch. Biochem. 23:96.

28. Christensen, H. N., Cushing, M. K. and Streicher, J. A. 1949 Concentration of Amino Acids by the Excised Diaphragm Suspended in Artificial Media. II. Inhibition of the Concentration of Glycine by Amino Acids and Related Substances. Arch. Biochem. 23:106.

29. Stern, J. R., Eggleston, L. V., Hems, R. and Krebs, H. A. 1949 Accumulation of Glutamic Acid in Isolated Brain Tissue. Biochem. J. 44:410.

30. Wiseman, G. 1953 Absorption of Amino-Acids Using an *In Vitro* Technique. J. Physiol. 120:63.

31. Fridhandler, L. and Quastel, J. H. 1955 Absorption of Amino Acids from Isolated Surviving Intestine. Arch. Biochem. Biophys. 56:424.

32. Christensen, H. N., Riggs, T. R. and Ray, N. E. 1952 Concentrative Uptake of Amino Acids by Erythrocytes in Vitro. J. Biol. Chem. 194:41.

33. Riggs, T. R., Christensen, H. N. and Palatine, I. M. 1952 Concentrating Activity of Reticulocytes for Glycine. J. Biol. Chem. 194:53.

34. Christensen, H. N., Riggs, T. R., Fischer, H. and Palatine, I. M. 1952 Amino Acid Concentration by a Free Cell Neoplasm: Relations Among Amino Acids. J. Biol. Chem. 198:1.

35. Christensen, H. N., Riggs, T. R., Fischer, H. and Palatine, I. M. 1952 Intense Concentration of α, γ-Diaminobutyric Acid by Cells. J. Biol. Chem. 198:17.

36. Eagle, H., Piez, K. A. and Levy, M. 1961 The Intracellular Amino Acid Concentrations Required for Protein Synthesis in Cultured Human Cells. J. Biol. Chem. 236:2039.

37. Hare, J. D. 1967 Location and Characteristics of the Phenylalanine Transport Mechanism in Normal and Polyona-Transformed Hamster Cells. Cancer Res. 27:2357.

38. Foster, D. O. and Pardee, A. B. 1969 Transport of Amino Acids by Confluent and Non-Confluent 3T3 and Polyoma Virus-Transformed 3T3 Cells Growing on Glass Cover Slips. J. Biol. Chem. 244:2675.

39. Isselbacher, K. J. 1972 Increased Uptake of Amino Acids and 2-Deoxy-D-glucose by Virus Transformed Cells in Culture. Proc. Nat. Acad. Sci. 69:585.

40. Inbar, M., Ben-Bassat, H. and Sachs, L. 1971 Location of Amino Acid and Carbohydrate Transport Sites in the Surface Membrane of Normal and Transformed Mammalian Cells. J. Memb. Biol. 6:195.

41. Burger, M. M. and Noonan, K. D. 1970 Restoration of Normal Growth by Covering of Agglutinin Sites on Tumor Cell Surface. Nature 228:512.

42. Sumner, J. B. 1919 The Globulins of the Jack Bean, Conavalia Ensiformis. J. Biol. Chem. 37:137.

43. Sumner, J. B. and Howell, S. F. 1936 The Identification of the Hemagglutinin of the Jack Bean with Concanavalin A. J. Bacteriol. 32:227.

44. Sumner, J. B., Gralén, N., and Eriksson-Quensel, I. B. 1938. The Molecular Weights of Canavalin, Concanavalin A and Concanavalin B. J. Biol. Chem. 125:45.

45. Olson, M. O. and Liener, I. E. 1967 Some Physical and Chemical Properties of Con A, the Phytohemagglutinin of the Jack Bean. Biochem. 6:105.

46. Agrawal, B. B. L. and Goldstein, I. J. 1967 Physical and Chemical Characterization of Concanavalin A, the Hemagglutinin from Jack Bean (Canavalia ensiformis). Biochim Biophys Acta 133:376.

47. Wang, J. L., Cunningham, B. A. and Edelman, G. M. 1971 Unusual Fragments in the Subunit Structure of Concanavalin A. Proc. Nat. Acad. Sci. 68:1130.

48. Abe, Y., Iwabuchi, M. and Ishii, S. 1971 Multiple Forms in the Subunit Structure of Concanavalin A. Biochem. Biophys. Res. Commun. 45:1271.

49. Yariv, J., Kalb, A. J. and Levitski, A. 1968 The Interaction of Concanavalin A with D-glucopyranoside. Biochim. Biophys. Acta 165:303.

50. Kalb, A. J. and Levitski, A. 1968 Metal-Binding Sites of Concanavalin A and their Role in the Binding of α-Methyl-D-glucopyranoside. Biochem. J. 109:669.

51. Waxdal, M. J., Wang, J. L., Pflumm, M. N. and Edelman, G. M. 1971 Isolation and Order of the Cyanogen Bromide Fragments of Concanavalin A. Biochem. 10:3343.

52. Hardman, K. D., Wood, M. K., Schiffer, M., Edmundson, A. B. and Ainsworth, C. F. 1971 Structure of Concanavalin A at 4.25-Ångstrom Resolution. Proc. Nat. Acad. Sci. 68:1393.

53. Quiocho, F. A., Reeke, G. N., Jr., Becker, J. W., Lipscomb, W. N. and Edelman, G. M. 1971 Structure of Concanavalin A at 4 Å Resolution. Proc. Nat. Acad. Sci. 68:1853.

54. Powell, A. E. and Leon, M. A. 1970 Reversible Interaction of Human Lymphocytes with the Mitogen Concanavalin A. Exp. Cell Res. 62:315.

55. Beckert, W. H. and Sharkey, M. M. 1970 Mitogenic Activity of the Jack Bean (Canavalia ensiformis) with Rabbit Peripheral Blood Lymphocytes. Int. Arch. Allergy 39:337.

56. Berlin, R. D. 1972 Effect of Concanavalin A on Phagocytosis. Nature, New Biol. 235:44.

57. Friberg, S. J., Cochran, A. J. and Golub, S. H. 1971 Concanavalin A Inhibits Tumor Cell Migration. Nature, New Biol. 232:121.

58. Goldstein, I. J., Hollerman, C. E. and Merrick, J. M. 1965 Protein-carbohydrate Interaction I. The Interaction of Polysaccharides with Concanavalin A. Biochim. Biophys. Acta 97:68.

59. Inbar, M. and Sachs, L. 1969 Interaction of the Carbohydrate-Binding Protein Concanavalin A with Normal and Transformed Cells. Proc. Nat. Acad. Sci. 63:1418.

60. Eckhart, W., Dulbecco, R. and Burger, M. M. 1971 Temperature-Dependent Surface Changes in Cells Infected or Transformed by a Thermosensitive Mutant of Polyoma Virus. Proc. Nat. Acad. Sci. 68:283.

61. Curtis, A. S. C. 1967 in The Cell Surface: Its Molecular Role in Morphogenesis, pp. 206, 211, 214, 238, 259 and 266. (Academic Press).

62. Ben-Bassat, H., Inbar, M. and Sachs, L. 1971 Changes in the Structural Organization of the Surface Membrane in Malignant Cell Transformation. J. Memb. Biol. 6:183.

63. Pardee, A. B. 1964 Cell Division and A Hypothesis of Cancer, Nat. Cancer Inst. Monograph 14:7.

64. Burger, M. M. 1969 A Difference in the Architecture of the Surface Membrane of Normal and Virally Transformed Cells. Proc. Nat. Acad. Sci. 62:994.

65. Aub, J. C., Tieslau, C. and Lankester, A. 1963 Reactions of Normal and Tumor Cell Surfaces to Enzymes. I. Wheat-Germ Lipase and Associated Mucopolysaccharides. Proc. Nat. Acad. Sci. 50:613.

66. Burger, M. M. and Goldberg, A. R. 1967 Identification of a Tumor-Specific Determinant on Neoplastic Cell Surfaces. Proc. Nat. Acad. Sci. 57:359.

67. Inbar, M. and Sachs, L. 1969 Structural Difference in Sites on the Surface Membrane of Normal and Transformed Cells. Nature 223:710.

68. Burger, M. M. 1970 in Proc. Intern. Conf. Biol. Membranes, Stresa (North-Holland Publishing Co.)

69. Burger, M. M. 1970 Proteolytic Enzymes Initiating Cell Division and Escape from Contact Inhibition of Growth. Nature 227: 170.

70. Ozanne, B. and Sambrook, J. 1971 Binding of Radioactively Labelled Concanavalin A and Wheat Germ Agglutinin to Normal and Virus-Transformed Cells. Nature, New Biol. 232:156.

71. Cline, M. J. and Livingston, D. C. 1971 Binding of ^{3}H-Concanavalin A by Normal and Transformed Cells. Nature, New Biol. 232: 155.

72. Nevo, A., DeVries, A. and Katchalsky, A. 1955 Interaction of Basic Polyamino Acids with Red Blood Cell. I. Combination of Polylysine with Single Cells. Biochim Biophys. Acta 17: 536.

73. Katchalsky, A., Danon, D., Nevo, A. 1959. Interactions of Basic Polyelectrolytes with the Red Blood Cell II. Agglutination of Red Blood Cells by Polymeric Bases. Biochim Biophys Acta 33:120.

74. Kornguth, S. E., Stahmann, M. A. and Anderson, J. W. 1961 Effect of Polylysine on the Cytology of Ehrlich Ascites Tumor Cells. Exp. Cell Res. 24:484.

75. Sirica, A. E. and Woodman, R. J. 1970 Aggregation of L1210 Leukemic Cells in Vitro by Chitosan and its Derivatives. Fed. Proc. 29:681.

76. Sirica, A. E. and Woodman, R. J. 1971 Selective Aggregation of L1210 Leukemia Cells by the Polycation Chitosan. J. Nat. Cancer Inst. 47:377.

77. Burger, L. W. C. and Stahmann, M. A. 1951 The Combination of Lysine Polypeptides with Tobacco Mosaic Virus. J. Biol. Chem. 193: 13.

78. Watson, D. W. and Bloom, W. L. 1952 Antimicrobial Activity of a Natural and A Synthetic Polypeptide. Proc. Soc. Exp. Biol. Med. 81:29.

79. Shalitin, C., Katchalski, E. 1957 The Inactivation of Bacteriophage T_2hr_1 by poly-L-lysine. Bul. Res. Council Israel, 6a:314.

80. Green, M. and Stahmann, M. A. 1953 Inhibition of Mumps Virus Multiplication by a Synthetic Polypeptide. Proc. Soc. Exp. Biol. Med. 83:852.

81. Rubini, J. R., Rasmussen, A. F., Stahmann, M. A. 1951. Inhibitory Effect of Synthetic Lysine Polypeptides on Growth of Influenza Virus in Embryonated Eggs. Proc. Soc. Exp. Biol. Med. 76:662.

82. Burger, W. C. and Stahmann, M. A. 1952. The Agglutination and Growth Inhibition of Bacteria by Lysine Polypeptides. Arch. Biochem. Biophys. 39:27.

83. Katchalski, E., Bichovsky, L. and Volcani, E. B. 1953 The Action of Some Water-Soluble Poly-α-Amino Acids on Bacteria. Biochem. J. 55:671.

84. Richardson, T., Hodgett, J., Lindner, A. and Stahmann, M. A. 1959 Action of Polylysine on Some Ascites Tumors in Mice. Proc. Soc. Exp. Biol. Med. 101:382.

85. Shah, V. C. and Reilly, P. 1967 Effect of Histones, Other Basic Proteins and Some Antibiotics on the Transplantability of Mouse Mammary Tumors. Nature 213:403.

86. Yarnell, M. M. and Ambrose, E. J. 1969 Studies of Tumor Invasion in Organ Culture. I. Effects of Basic Polymers and Dyes on Invasion and Dissemination. Europ. J. Cancer 5:255.

87. Ambrose, E. J., Easty, D. M. and Jones, P. C. T. 1958. Specific Reactions of Polyelectrolytes with the Surfaces of Normal and Tumor Cells. Brit. J. Cancer 12:439.

88. Larsen, B. and K. Olsen 1968 Inhibitory Effect of Polycations on the Transplantability of Mouse Leukemia Reversed by Heparin. Europ. J. Cancer 4:157.

89. Mangos, J. A. and McSherry, N. R. 1968 Studies on the Mechanism of Inhibition of Sodium Transport in Cystic Fibrosis of the Pancreas. Pediat. Res. 2:378.

90. Ryser, H. J. P. 1967 A Membrane Effect of Basic Polymers Dependent on Molecular Size. Nature 215:934.

91. Ryser, H. J. P. and Hancock, R. 1965 Histones and Basic Polyamino Acids Stimulate the Uptake of Albumin by Tumor Cells in Culture. Science 150:501.

92. Sanders. E. J. and Bell, L. G. E. 1970 Some Physiological and Morphological Effects of Polylysine on Amoeba Proteus. J. Cell Sci. 7:739.

93. Lenard, J. and Singer, S. J. 1966 Protein Conformation in Cell Membrane Preparations as Studied by Optical Rotatory Dispersion and Circular Dichroism. Proc. Nat. Acad. Sci. 56:1828.

94. Liley, A. W. 1956 An Investigation of Spontaneous Activity at the Neuromuscular Junction of the Rat. J. Physiol. 132:650.

95. Dulbecco, R. and Vogt, M. 1954 Plague Formation and Isolation of Pure Lines with Poliomyelitis Viruses. J. Exp. Med. 99: 167.

96. Hanks, J. H. and Wallace, R. E. 1949 Relation of Oxygen and Temperature in the Preservation of Tissues by Refrigeration. Proc. Soc. Exp. Biol. Med. 71:196.

97. Merchant, D. J., Kahn, R. H. and Murphy, W. H. 1967 in Handbook of Cell and Organ Culture. pp. 240 (Burgess Publishing Co.)

98. Chowdhury, T. K. 1969 Fabrication of Extremely Fine Glass Micropipette Electrodes. J. Sci. Instruments (J. Physics E) 2: 1087.

99. Chowdhury, T. K. 1969 Origin of the Tip Potential in Fine-tipped Glass Microelectrodes. Biophys. J. 9:A-39.

100. Byzov, A. L. and Chernyshov, V. I. 1961 Machine for Making Microelectrodes. Biophysics 6 (4):79.

101. Lowry, O. H., Rosenbrough, N. J., Farr, A. L. and Randall, R. J. 1951 Protein Measurement with the Folin phenol Reagent. J. Biol. Chem. 193:265.

102. Dunn, O. J. 1964 in Basic Statistics: A Primer for the Biomedical Sciences, pp. 78 (John Wiley & Sons, Inc.)

103. Dunn, O. J. 1964 in Basic Statistics: A Primer for the Biomedical Sciences pp. 190, (John Wiley & Sons, Inc.)

104. Balitsky, K. P. and Shuba, E. P. 1964 Resting Potential of Malignant Tumor Cells. Acta Unio Intern. Contra Cancrum 20: 1391.

105. Schanne, O. 1960 Das Verhalten des Membranpotentials von Zellukulturen unter besonderer Berücksichtgung Malignen Gewebes. Z. Biol. 112:234.

106. So, L. L. and Goldstein, I. J. 1968 Protein-Carbohydrate Interaction. XIII. The Interactions of Concanavalin A with α-Mannans from a Variety of Microorganisms. J. Biol. Chem. 243:2003.

107. Mallucci, L. 1971 Binding of Concanavalin A to Normal and Transformed Cells as Detected by Immunofluorescence. Nature, New Biol. 233:241.

108. Nicolson, G. L. 1971 Difference in Topology of Normal and Tumour Cell Membranes Shown by Different Surface Distributions of Ferritin-conjugated Concanavalin A. Nature, New Biol. 233: 244.

109. Dainty, J. 1962 Ion Transport and Electrical Potentials in Plant Cells. Ann. Rev. Plant Physiol. 13:379.

110. Goldman, D. E. 1943 Potential, Impedance, and Rectification in Membranes. J. Gen. Physiol. 27:37.

APPENDIX

Since amino acids are amphoteric in nature, they can exist either in the charged form or in the neutral form depending on the pH of the solution. From the Henderson-Hasselbalch equation, $pH - pK + \log \frac{[A^-]}{[HA]}$, where $[A^-]$ is the concentration of the basic form and [HA] is the concentration of the acid, the ratio of these two forms can be estimated. At pH 7.0, glycine and phenylalanine are present predominantly in the neutral form only, with 0.12% and 8% in the respective monoanionic forms. On the other hand, 50% of histidine exist in the neutral form and the other 50% in monocationic form. With the assumption that the membrane is simply a interfacial boundary between the extra- and intracellular fluids, the unidirectional flux of a passively diffusing neutral substance follows Fick's law:

$$J_{I \rightarrow II} = PC_I = \frac{1}{X} DC_I$$

where $J_{I \rightarrow II}$ is the unidirectional flux of the uncharged permeant from side I to side II, in this case from extracellular to intracellular space. P is the permeability coefficient and D is the diffusion coefficient. C denotes the concentration and X the thickness of the membrane. The physical interpretation of the diffusion coefficient is presented by Stokes Einstein relationship:

$$D = \frac{KT}{6\pi r\eta}$$

where K is Boltzmann's constant, and T the absolute temperature. η denotes viscosity of the solvent and r the radius of the particle. Therefore, the flux is expressed by the following equation:

$$J_{I \rightarrow II} = \frac{1}{X} \cdot \frac{KT}{6\pi r\eta} C_I$$

When temperature is changed, the thickness of the membrane, viscosity of the solvent and radius of the permeant molecule are assumed to be unaltered. Thus, the ratio of the fluxes at two different temperatures is directly proportional to the ratio of the two absolute temperatures, namely,

$$\frac{J_{I\rightarrow II}(T')}{J_{I\rightarrow II}(T)} = \frac{T'}{T}$$

Therefore, the Q_{10} at 27°C is $\frac{J_{I\rightarrow II}(310)}{J_{I\rightarrow II}(300)} = \frac{310}{300} = 1.03$

On the other hand, for some charged species, the flux will be determined both by the concentration and by the intracellular potential which is -5.0 mV in this case. According to Dainty's formulation (109) of the Goldman equation (110), the monocationic unidirectional influx is given by:

$$J_{I\ II} = -P\ \frac{EF/RT}{1-e^{EF/RT}}\ C_I = -\frac{D}{X}\cdot\frac{EF/RT}{1-e^{EF/RT}}\ C_I = -\frac{KT}{6\pi r\eta x}\ \frac{EF/RT}{1-e^{EF/RT}}\ C_I$$

F is the Faraday constant, E the intracellular potential, and R the gas constant. The Q_{10} at 27°C can be calculated as follows:

$$Q_{10} = \frac{J_{I\rightarrow II}(310)}{J_{I\rightarrow II}(300)} = \frac{\frac{K(310)(EF/310R)}{6\pi r\eta x(1-e^{EF/310R})}}{\frac{K(300)(EF/300R)}{6\pi r\eta x(1-e^{EF/300R})}} = \frac{310(EF/310R)(1-e^{EF/300R})}{300(EF/300R)(1-e^{EF/310R})}$$

$$= \frac{1-e^{EF/300R}}{1-e^{EF/310R}} = \frac{1-e^{-5F/300R}}{1-e^{-5F/310R}} = \frac{0.0817}{0.0792} = 1.03$$

Therefore, if passive diffusion is responsible for the uptake of glycine, phenylalanine and histidine, the Q_{10} values should be 1.03 no matter whether the molecules are present as neutral species or monocationic ions. The experimental values of Q_{10} are 1.31, 1.42 and 1.18 for glycine, phenylalanine and histidine respectively, indicating that

perhaps some active transport process is involved in the uptake of these three amino acids in the cancer cells.